Biochimica et Biophysica Acta 1840 (2014) 667–680

Contents lists available at ScienceDirect

Biochimica et Biophysica Acta

journal homepage: www.elsevier.com/locate/bbagen

CD1d favors MHC neighborhood, GM_1 ganglioside proximity and low detergent sensitive membrane regions on the surface of B lymphocytes

Dilip Shrestha [a], Mark A. Exley [c], György Vereb [a,b], János Szöllősi [a,b,*], Attila Jenei [a]

[a] Department of Biophysics and Cell Biology, Medical and Health Science Center, University of Debrecen, Nagyerdei krt. 98, 4032 Debrecen, Hungary
[b] MTA-DE Cell Biology and Signaling Research Group, University of Debrecen, Nagyerdei Krt. 98, 4032 Debrecen, Hungary
[c] Brigham and Women's Hospital, Harvard Medical School, Boston, MA, USA

ARTICLE INFO

Article history:
Received 19 June 2013
Received in revised form 15 October 2013
Accepted 18 October 2013
Available online 26 October 2013

Keywords:
CD1d
MHC
Rafts
FRET
Methyl-β-cyclodextrin
Simvastatin

ABSTRACT

Background: Cluster of differentiation 1 (CD1) represents a family of proteins which is involved in lipid-based antigen presentation. Primarily, antigen presenting cells, like B cells, express CD1 proteins. Here, we examined the cell-surface distribution of CD1d, a subtype of CD1 receptors, on B lymphocytes.
Methods: Fluorescence labeling methods, including fluorescence resonance energy transfer (FRET), were employed to investigate plasma membrane features of CD1d receptors.
Results: High FRET efficiency was observed between CD1d and MHC I heavy chain (MHC I-HC), β_2-microglobulin (β_2m) and MHC II proteins in the plasma membrane. In addition, overexpression of CD1d reduced the expression of MHC II and increased the expression of MHC I-HC and β_2m proteins on the cell-surface. Surprisingly, β_2m dependent CD1d isoform constituted only ~15% of the total membrane CD1d proteins. Treatment of B cells with methyl-β-cyclodextrin (MβCD) / simvastatin caused protein rearrangement; however, FRET demonstrated only minimal effect of these chemicals on the association between CD1d and GM_1 ganglioside on cell-surface. Likewise, a modest effect was only observed in a co-culture assay between MβCD/simvastatin treated C1R–CD1d cells and invariant natural killer T cells on measuring secreted cytokines (IFNγ and IL4). Furthermore, CD1d rich regions were highly sensitive to low concentration of Triton X-100. Physical proximity between CD1d, MHC and GM_1 molecules was also detected in the plasma membrane.
Conclusions: An intricate relationship between CD1d, MHC, and lipid species was found on the membrane of human B cells.
General significance: Organization of CD1d on the plasma membrane might be critical for its biological functions.

1. Introduction

Antigen presentation is a defining mechanism in the adaptive immune system. While several decades of information are available about peptide antigen presentation, through major histocompatibility complex (MHC) molecules, in the activation of conventional T cells, similar roles of lipids in antigen presentation have gained significant attention beginning only in the last couple of decades [1–3]. The non-polymorphic transmembrane glycoproteins known as Cluster of Differentiation (CD1) were found to present these non-peptide antigens to a distinct subset of T cells [3,4]. In fact, these CD1 molecules, encoded on human chromosome 1, resemble MHC I heavy chain (MHC I-HC) in physical structure [3,5–7] and MHC II molecules in function, mainly endosomal surveillance [6,8], thus possessing an admixture of features which have led to the hypothesis that these molecules have diverged from a common ancestral gene. Interestingly, MHC I and CD1d also share the chaperones, calnexin and calreticulin, which are important for their appropriate folding [9,10]. In human, CD1 a, -b and -c molecules are placed in group I CD1 while CD1d is kept separately in group II [7,10,11]. CD1d- restricted natural killer T (NKT) cells release copious amount of both Th1 and Th2 type cytokines and chemokines upon engagement with CD1d receptors, underscoring the roles of CD1d in immunoregulation [12,13]. Most earlier studies demonstrated the trafficking behavior of CD1 from the plasma membrane to the intracellular endosomal membrane compartment and vice versa [4,6,14–21]; these studies provided evidence that CD1 molecules sample antigens in the endocytic system but the membrane organization of these receptors which could influence such biological behaviors of these molecules has not been explored in detail yet. Furthermore, owing to the broad role played by CD1d in B lymphocytes, which came into prominence recently due to its role in sustaining antibody responses [22,23] and for the maintenance of invariant natural killer T

Abbreviations: MHC, major histocompatibility complex; CD1, cluster of differentiation 1; NKT cells, natural killer T cells; iNKT, invariant natural killer T cells; β_2m, β2-microglobulin; MβCD, methyl-β-cyclodextrin; FRET, fluorescence resonance energy transfer; NCS, newborn calf serum; Mabs, monoclonal antibodies; TfR, transferrin receptor; FCET, flow-cytometric FRET; CTxB, cholera toxin subunit B; FCDR test, flow cytometric detergent resistance test; TX100, Triton X-100; DRMs, Detergent resistant membrane regions; PBMC, peripheral-blood mononuclear cells; α-gal, α-galactosylceramide; APC, Antigen presenting cell

* Corresponding author at: Department of Biophysics and Cell Biology, Medical and Health Science Center, University of Debrecen, Nagyerdei krt 98, Debrecen 4032, Hungary. Tel.: +36 52 412 623; fax: +36 52 532 201.
E-mail address: szollo@med.unideb.hu (J. Szöllősi).

0304-4165/$ – see front matter © 2013 Elsevier B.V. All rights reserved.
http://dx.doi.org/10.1016/j.bbagen.2013.10.030

(iNKT) cells [24], we focused our studies on this molecule, which is also the only CD1 isoform expressed by mouse [7,25]. Two isoforms of CD1d have been observed on the surface of cells: one that is physically bound to β2-microglobulin (β_2m) and the other that is independently present without β_2m [11,26]. Hereon, we will address these isoforms as β_2m-dependent and β_2m-independent CD1d proteins. Biochemical studies also illustrated that CD1d is in association with MHC II molecules in the plasma membrane [25] and with invariant chain in membrane-bound intracellular compartments [27]. These observations suggested that these molecules might be in close vicinity of each other and most probably in some specific domains like lipid-rafts. In a murine cell line system, CD1d was distinctly found to be located in the lipid-rafts and the disruption of lipid-rafts by methyl-β-cyclodextrin (MβCD) was found to interfere with the NKT cell activational responses [28–31]. Furthermore, we reported the co-existence of MHC I and MHC II in nanodomains of various types of cells using fluorescence resonance energy transfer (FRET) [32–36] and electron microscopy [33]. Since, co-immunoprecipitation was mainly used to detect protein–protein interactions in the case of CD1d, even for the membrane fractions, which can present artefactual interactions and is difficult to reproduce, we thought to utilize FRET, which can demonstrate physiological and dynamic interactions and is a better approach to investigate the distribution of CD1d proteins in the plasma membrane. FRET is very sensitive to changes in distance because the rate of energy transfer is inversely proportional to the sixth power of the distance separating the donor and acceptor fluorophores. This sensitivity to distance makes FRET a useful tool for investigating protein–protein interactions within the range of 1–10 nm. In this study, we demonstrate that CD1d proteins are indeed proximal to MHC proteins and are present in detergent sensitive domains of the membrane in lymphocytes. Surprisingly, β_2m dependent CD1d comprised only a small fraction of CD1d proteins on the membrane (~15%). We also noted that CD1d rich regions were mildly affected by cholesterol modulation, but were significantly altered by low concentration of Triton X-100 (TX100). Likewise, a co-culture assay between C1R–CD1d and iNKT cells also demonstrated the partial dependence of CD1d rich regions on cholesterol. In summary, CD1d seems to have an intricate relationship with MHC proteins and membrane lipids, and it also can apparently form larger protein–protein or protein–lipid complexes in the membrane of C1R–CD1d cells.

2. Materials and methods

2.1. Cell lines

The HLA-C expressing mutant B lymphoid cell line, C1R [37], stably expressing full-length CD1d was used in this study. The characterization of this cell line, including transfection details has been described elsewhere [38]. To obtain cells with uniform CD1d expression, the transfected C1R cells were magnetically sorted using 27.1.9 CD1d antibody and pan anti-mouse secondary antibody conjugated magnetic Dynabeads (Life Technologies/Invitrogen, Budapest, Hungary) following the manufacturer's instructions. Once sorted, the cells were referred to as C1R–CD1d. The cells were grown in RPMI media containing 10% newborn calf serum (NCS), with the inclusion of drug G418 at 300 μg/ml concentration unless stated otherwise.

2.2. Antibodies

The following monoclonal antibodies (Mabs) were used: the pan-MHC-I W6/32 (recognizes MHC I-HC associated with β_2m, IgG2a) [39,40] , HC-10 (recognizes free MHC I-HC, IgG2a) [40–43], L368 (anti-β_2m, IgG1) [44], L243 (anti-MHC-DR, IgG2a) [45], OKT9 (anti-transferrin receptor (TfR), IgG1) [46], 51.1.3 (anti-CD1d, IgG2b) and 27.1.9 (anti-CD1d, IgG1) [47]. Antibodies were prepared from hybridoma supernatants according to the standard protocol by Sepharose A affinity chromatography. Antibodies were coupled to Alexa 546- and Alexa 647-succinimidyl ester dyes following the manufacturer's instructions (Molecular Probes, Invitrogen) and the dye to protein ratios were calculated based on the spectrophotometric absorbance values of the proteins. MEM75 antibody, against TfR [48] was a kind gift from Václav Horejsí (Institute of Molecular Genetics, Academy of Sciences, Prague, Czech Republic).

2.3. Cell labeling

For each sample, approximately one million freshly harvested cells were taken in 50 μl volume of PBS buffer (pH 7.4) containing 1 mg/ml BSA and 0.01% sodium azide. A saturating concentration of the dye conjugated antibodies was added to these cells, and the mixed suspension was incubated in a dark environment for 30 min on ice. After the incubation, these cells were washed twice with ice-cold PBS buffer in order to remove unbound antibodies. Finally, the cells were suspended in 1% formaldehyde solution, and they were kept at 4 °C until the measurements were performed in a flow cytometer or a confocal microscope.

2.4. Quantitation of membrane receptors

In order to determine the expression level of each of the receptors, QIFIKIT (Dako Cytomation, Glostrup, Denmark) was used according to the manufacturer's instructions. QIFIKIT is an indirect immunofluorescence based method of determining antigen density per cell by flow cytometry. This consists of a series of beads coated with known quantities of Mabs which emulate cells with defined antigen densities. Specimen cells were labeled with the primary mouse Mab at saturating concentration. Then, the cells were incubated, in parallel with the QIFIKIT beads, with FITC dye tagged polyclonal anti-mouse secondary F(ab′)$_2$. Finally, a calibration curve was plotted between the fluorescence intensity of the individual bead populations against the number of Mab molecules on these beads. This curve was then used for determining the number of receptors on the specimen cells by interpolation. For our purpose, fluorescence intensities were measured on a FACSCalibur instrument using a 530 +/− 30 BP filter.

2.5. Confocal microscopy

A Zeiss LSM 510 confocal laser scanning microscope (Carl Zeiss AG, Jena, Germany) with a Plan-Apochromat 40× (NA = 1.2) water immersion objective was used to record the images. An optical slice (512 × 512-pixels) of 1.5 μm thickness, four-times averaged, was taken from the top of a cell for co-localization experiments. Simultaneously, a multitrack option of the microscope was used to acquire images to avoid any possible crosstalk between the detection channels.

2.6. Co-localization study of the receptors

The spatial proximity of membrane proteins was studied by image cross-correlation method at ~200 nm scale. For this purpose, cells were doubly or triply labeled with markers specific for distinct molecular species but tagged with spectrally different fluorophores. Images were acquired from the top of the cells as a horizontal optical slice by confocal microscope. A custom program written in LABVIEW platform was used for the computational analysis of the cross-correlation coefficient (C) from the image pairs [49,50]. For an image pair 'x' and 'y', the image cross-correlation coefficient was calculated by the following formula:

$$C = \frac{\sum_i \sum_j \left(x_{i,j} - \langle x \rangle\right)\left(y_{i,j} - \langle y \rangle\right)}{\sqrt{\sum_i \sum_j \left(x_{i,j} - \langle x \rangle\right)^2 \sum_i \sum_j \left(y_{i,j} - \langle y \rangle\right)^2}}$$

where $x_{i,j}$ and $y_{i,j}$ are fluorescence pixel values at co-ordinates *i* and *j* in images *x* and *y*. Only those pixels that were above the detection threshold in both images were used for analysis. The theoretical maximum is '1' for perfect overlap of proteins (i.e. 100% co-localization); while a value '0' implies random overlap of proteins and a negative value '−1' indicates an anti-colocalized situation of the two molecules where a pixel is bright in one channel and dim in the other.

2.7. Flow-cytometric FRET (FCET) experiments

FCET experiments were carried out using FACSArray flow cytometer (Becton Dickinson, Franklin Lakes, and NJ) equipped with 532 and 633 nm lasers. For this purpose, samples were either singly or doubly labeled with Alexa-546, Alexa-555 or Alexa-647 dye conjugated probes and/or antibodies serving as donor and acceptor molecules. Emitted signals due to 532 laser excitation were collected in the donor (575 +/− 25) and the transfer (650 LP) channels while the 633 nm laser excited the acceptor dyes and the signals were collected in the acceptor channel (650 +/− 10). The obtained FCS data were analyzed using the ReFleX software [51]. The mean FRET efficiencies were then calculated from roughly 20,000 cells. For two-color three-protein FCET experiment, similar protocol was used as above except the inclusion of the third protein as a donor or as an acceptor. The conventional FRET has two proteins as a FRET pair but this modified two-color three-protein FRET has three proteins as FRET pair, and two of these proteins are combinedly used as a donor or acceptor molecules. This means two Mabs against two receptors are conjugated to same Alexa dyes separately. However, they are mixed during cell-labeling and are used as either donor or acceptor. Thus, two Mabs conjugated to same Alexa dyes behave together as a unit representing either donor or acceptor species.

2.8. CD1d and GM_1 ganglioside association

Cholera toxin subunit B (CTxB) was used to visualize GM_1 gangliosides and 27.1.9 CD1d Mab was used to identify CD1d proteins. For co-localization assay, the experiments were performed using the confocal microscope as described above, after labeling each of the species in the membrane of the cells. Alexa 488 conjugated CTxB was excited by 488 nm laser and the signals were detected through a 505/550 nm BP filter while Alexa 647 conjugated CD1d antibody was excited by 632 nm laser and the fluorescence emission was detected through 650 LP filter. For the FCET experiment, Alexa 555-CTxB (Invitrogen) was used as a donor, while Alexa 647–27.1.9 CD1d Mab was used as an acceptor and the measurements were performed in FACSArray.

2.9. Flow cytometric detergent resistance (FCDR) test

For the kinetic assessment of CD1d enriched membrane regions, an earlier published protocol based on flow cytometry was followed [52]. Briefly, cells were labeled with Alexa 488 dyes conjugated Mabs or probes in 50 μl volume of PBS buffer (pH 7.4) containing 1 mg/ml BSA. The incubation and washing of the samples were carried out in a similar fashion as described for other samples in the labeling method. Importantly, formaldehyde fixation of cells was not done in this experiment. Measurements were carried out immediately after the sample preparation using 530 +/− 30 BP filter in FACScan instrument. At first, fluorescence intensities were recorded without TX100 from all samples (~50 s), thereafter, various concentrations of ice-cold TX100 was added to the sample swiftly. It was mixed for a few seconds and the measurements were continued for an additional 5 min. The FCS data were analyzed using ReFleX software. Later, SigmaPlot Version 10 was used to plot the graph of fluorescence intensity versus time using calculated data from ReFleX software.

2.10. Treatment of cells with methyl-β-cyclodextrin (MβCD) or simvastatin

Simvastatin and MβCD were purchased from Sigma, and the solutions were made as per the instructions from the company. For experimental purposes, simvastatin was also activated by hydrolysis at alkaline pH using sodium hydroxide following the manufacturer's specifications. Micromolar (μM) concentration of preactivated simvastatin was used to treat 3–10 million cells in 1% NCS RPMI media for 48 h at 37 °C in a humidified incubator with a constant supply of air with 5% CO_2. For MβCD treatment, 5–10 million cells, which were cultured in 1% NCS, unless otherwise mentioned, were taken in 1 ml of 0.1% NCS RPMI media and were incubated with 2 mM MβCD for 40 min or 10 mM MβCD for 15 min at 37 °C. Once the incubation was over, in both the cases, cells were washed extensively and labeled following the protocol described above.

2.11. Isolation of iNKT cells from peripheral blood mononuclear cells (PBMC)

PBMC were isolated from human peripheral blood by standard procedure using Ficoll density gradient centrifugation (Sigma). Thereafter, iNKT cells were separated from PBMC using human anti-iNKT magnetic beads (Miltenyi Biotec, Bergisch-Gladbach, Germany). Sorted iNKT cells were grown in flat bottomed 96 well plates, which contained α-galactosylceramide (α-gal, Avanti Polar Lipids, Inc., Alabama, USA) loaded mitomycin-arrested (50 μg/ml for 45 min) C1R–CD1d cells in GIBCO OpTmizer™ CTS™ T-Cell Expansion SFM media (Invitrogen). The medium was also supplemented with 5% AB human serum (Sera Laboratories International Ltd, West Sussex, UK), 200 ng/ml of recombinant IL2 (Shenandoah Biotechnology, Inc., USA) and 2 μg/ml phytohemagglutinin M (PHA-M, Sigma). Growth of the cells was carefully monitored over the days with clusters of cells indicating the survival and proliferation of iNKT cells. The concentration of IL2 was also gradually decreased from 200 ng/ml to 20 ng/ml (~10 U/ml) during the period of culture. The expanded iNKT cells had a high purity of >98% when examined by flow cytometry with C21 (anti-Vβ11, IgG2a, Beckman coulter), and OKT3 (anti-CD3, IgG2a).

2.12. iNKT cell activation assay

To determine the effect of membrane cholesterol depletion of C1R–CD1d cells in iNKT cell activation, a co-culture assay was also designed. In the case of simvastatin study, α-gal (250 ng/ml) was added to the cells only 4 h prior to the completion of 48 h of simvastatin incubation, whereas, α-gal was fed to cells for 18 h in the case of MβCD study. Cells for simvastatin treatment were grown in 1% NCS RPMI medium whereas for MβCD study were cultured in 10% NCS RPMI medium. C1R–CD1d cells were treated either with simvastatin or MβCD as described above in the treatment section. Once the reagent treatment was over, B cells were fixed with 1% formaldehyde for 20 min on ice and were extensively washed, in order to prevent the reassembly of cholesterol in the membrane. In the assay, 60,000 C1R–CD1d cells and 20,000 iNKT cells were seeded in each well of the round-bottomed 96 well plates with RPMI medium containing 5% human serum and 20 ng/ml recombinant IL2 for 48 h at 37 °C. Experiments were performed in triplicates for each test. Importantly, iNKT cells were grown in 5% human serum and 20 ng/ml recombinant IL2 containing RPMI medium for at least 48 h before it was used for the experiments.

2.13. Statistical analysis

For comparison, either an unpaired *t*-test or one-way ANOVA together with Tukey posthoc analysis was performed using SigmaStat 3.5 (GmbH, Germany) depending on the number of groups. Only '*p*' values <0.05 were considered significant. Non significant '*p*' values are indicated by abbreviation 'N.S.', whereas, '*p*' values <0.05, <0.005, and <0.0005 are denoted with *, **, and ***, respectively on the figures.

3. Results

3.1. Expression level of MHC I-HC, β2m, MHC II and CD1d in C1R–CD1d cells

We wanted to evaluate the relationship of CD1d with MHC proteins on the membrane of B lymphocytes. For this objective, we selected a B lymphoid cell-line, C1R–CD1d which was used in various pull-down experiments previously in an attempt to identify protein interaction partners of CD1d from both plasma membrane and intracellular compartments [10,11,25]. First, we examined the level of expression of various receptors on this cell-line by flow cytometry. As depicted in Fig. 1, MHC II was found to be the highest in expression followed by CD1d while MHC I-HC was almost three and half-fold lower in expression in comparison with MHC II in this cell line. Interestingly, the data obtained from the fluorescently labeled C1R–CD1d cells, after taking into account dyes-to-antibody ratios, also suggested that the membrane expression of β2m was higher than that of MHC I-HC molecules (Fig. 1).

3.2. Quantitative determination of surface receptors

Fluorescence signals obtained using dye-conjugated antibodies are relative instead of quantitative indicators of the expression level of proteins. Therefore, we calculated the number of MHC I-HC, β2m, MHC II and CD1d proteins on the membrane of C1R–CD1d cells using QIFIKIT (Fig. 1b). In agreement with the flow cytometric fluorescence histograms, MHC II was found to be the most abundant protein in the membrane of C1R–CD1d cells. Likewise, expression of β2m was also higher, approximately by 18,000 molecules/cell, in comparison to that of MHC I-HC. MHC I-HC forms a pair with β2m, a conformation detected by W6/32 antibody [40], and is also known to form self-clusters (oligomers) [33,53]. Therefore, typically the expression of MHC I-HC is higher than that of β2m proteins in most cells [33]. Hence, in order to identify the possibility of β2m free unpaired MHC I-HC molecules, we used a HC-10 antibody, which mainly recognizes HLA-B and -C isoforms of β2m free MHC I [40]. Using these antibodies, we found that there were only a few hundreds of β2m free MHC I-HC molecules on the surface of C1R–CD1d cells. Similarly, two antibodies, 27.1.9 and 51.1.3 hybridoma clones, against CD1d protein demonstrated comparable surface expression for CD1d proteins (Fig. 1b). Thus, in light of the numerical data, we concluded that β2m is definitely greater in numbers than MHC I-HC and abundant β2m independent CD1d is present on the membrane of C1R–CD1d cells.

3.3. CD1d expression affects expression of membrane MHC proteins

During the period of continuous growth, C1R–CD1d cells had the tendency of losing the membrane expression of CD1d; hence, giving rise to CD1d positive (CD1d +ve) and negative (CD1d −ve) population of C1R cells (Fig. 2a). We realized that such a phenomenon can be used to determine the effect of CD1d in the membrane expression of MHC and β2m proteins. Therefore, we compared the surface expression of these proteins in these two sub-groups. As expected, we observed marked differences in the expression of these proteins in C1R–CD1d "+ve" and C1R–CD1d "−ve" cells. β2m expression increased significantly in C1R–CD1d "+ve" cells (~46.7 ± 11.5%) in comparison to that of its expression in C1R–CD1d "−ve" cells thus confirming the role of CD1d in influencing the membrane expression of β2m. In addition, we also observed an increase in the expression of MHC I-HC (~10 ± 2.6%) and decrease in the expression of MHC II (~31.8 ± 4.6%) proteins in the plasma membrane of C1R-CD1d "+ve" cells in comparison with its C1R–CD1d "−ve" counterparts (Fig. 2b). The comparison of the expression of these proteins between C1R-Mock cells and C1R–CD1d cells also revealed a similar pattern (data not shown).

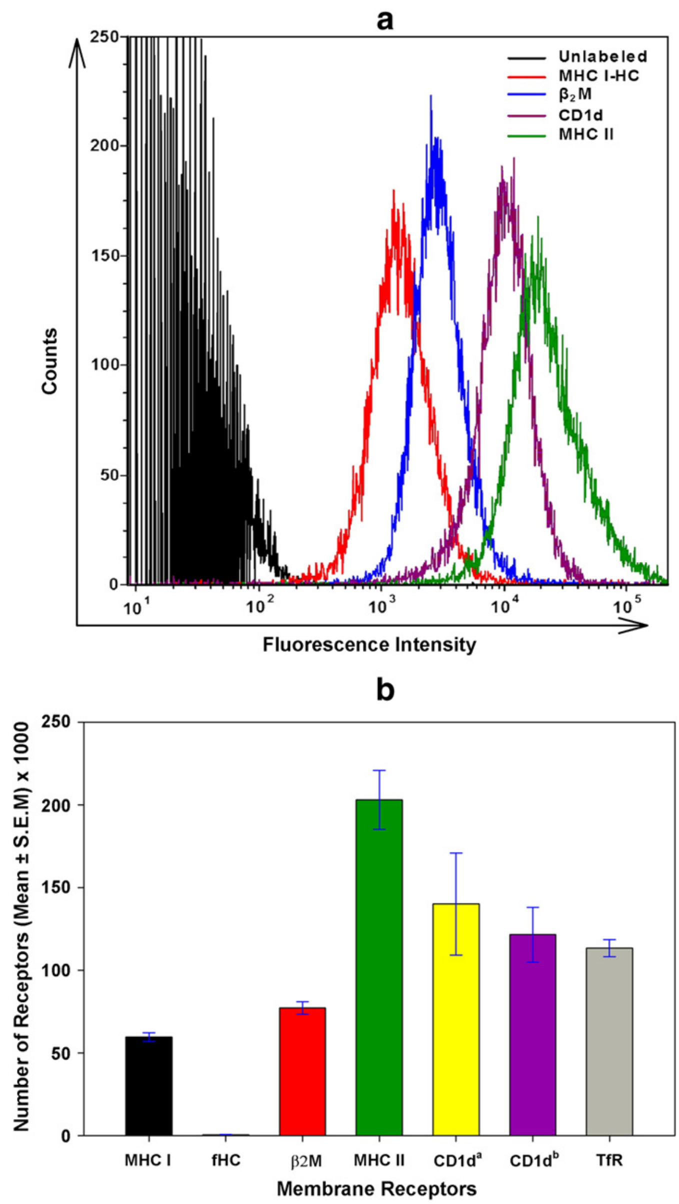

Fig. 1. a) Comparison of expression of various proteins on the surface of C1R–CD1d cells: C1R–CD1d cells were labeled with A647 dye conjugated specific Mabs against MHC I-HC (W6/32) red, β2m (L368) blue, CD1d (27.1.9 clone) violet, MHC II (L243) green following protocols described in the Materials and methods section independently. Measurements were performed using a FACSArray flow cytometer. b) QIFIKIT estimation of the number of membrane receptors: Cells were labeled according to the protocols provided by the manufacturer. Briefly, cells were labeled separately with unconjugated antibodies specific for each receptor. The mixture of cells and antibodies were incubated on ice for 30 min. The membrane receptors were saturated with antibodies, then, washing was done using ice-cold PBS buffer. Next, the samples were incubated with FITC conjugated F (ab′) $_2$ for 30 min on ice and in a dark environment. Finally, after washing twice with ice-cold PBS buffer, samples were fixed using 1% formaldehyde. The sample measurements were performed immediately by FACSCalibur. The numbers of receptors are presented as Mean ± S.E.M. In the figure, CD1d^a and CD1d^b indicate staining of CD1d receptors by 51.1.3 and 27.1.9 CD1d Mabs respectively.

3.4. Co-localization study of MHC I-HC, β2m, MHC II and CD1d in C1R–CD1d cells

Previous studies documented that a lot of common features existed between CD1d and MHC molecules, including antigen presenting characteristics [10,11,25]. Since MHC I and MHC II molecules extensively co-localize in the plasma membrane [32,33,53], we hypothesized that these molecules might be in the vicinity of CD1d as well. Alexa 546 and Alexa 647 dyes conjugated to the same L243 antibody

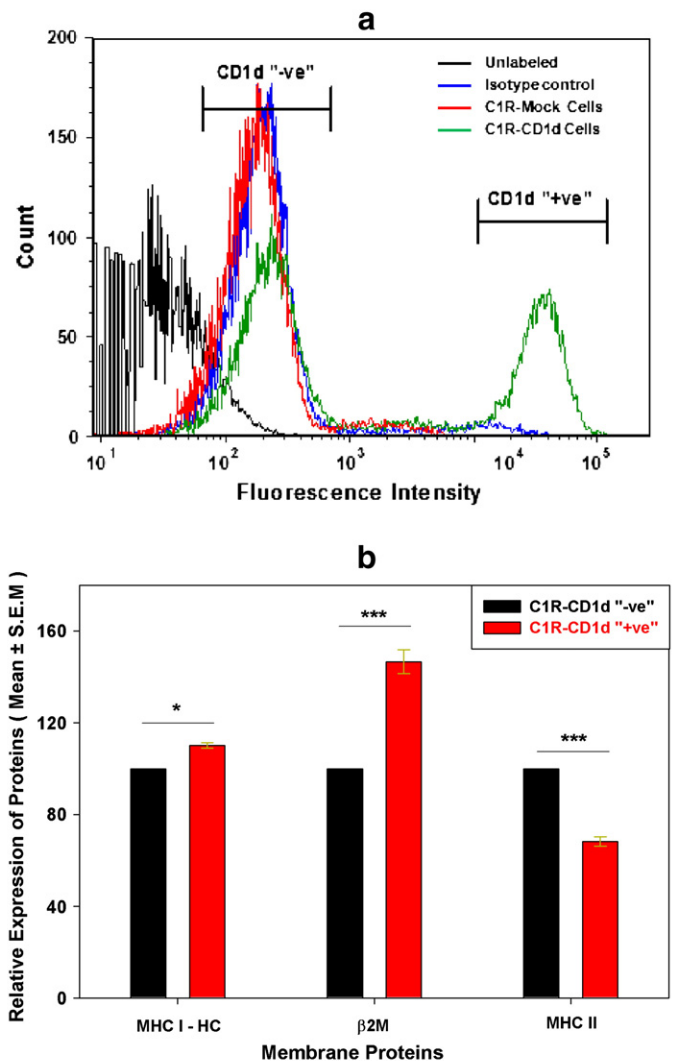

Fig. 2. CD1d expression affects expression of membrane MHC proteins: a) Histograms displaying fluorescence intensities from C1R cells with the following labeling parameters: Unlabeled (Black), Isotype control (Blue), C1R-Mock cells incubated with CD1d antibody (Red) and C1R cells containing C1R–CD1d "+ve" and C1R–CD1d "−ve" cells (Green). A 4D5 antibody, IgG1, against ErbB2 protein – an antigen over expressed in breast cancer cells – was used as an isotype control, where as 27.1.9 CD1d antibody was used to determine CD1d expression in C1R cells. Both the antibodies were conjugated to Alexa 647 dyes. b) The panel shows the change in fluorescence signals in percentage (Mean ± S.E.M.) in C1R–CD1d "+ve" population in comparison with a C1R–CD1d "−ve" population. The expression of receptors by C1R–CD1d "−ve" population was taken as 100%. A dual labeling of receptors of interest was carried out simultaneously as described in the Materials and methods section. One of the labeled receptors was always CD1d protein while the second receptor was among MHC I-HC, β_2m or MHC II proteins. Measurements were performed by a FACSCalibur instrument equipped with blue, 488 nm Ar ion laser, and red, 635 nm diode laser. Positive and negative populations for CD1d protein were gated carefully, and the fluorescence signals for each of the receptors in each population were quantified. Alexa 488 and Alexa 647 dyes conjugated antibodies were used in this experiment to avoid possible spectral overlap between dyes. In the figure, ⁎, and ⁎⁎⁎ indicate 'p' values <0.05, and <0.0005 respectively.

were used as a positive control, whereas, GM_1 ganglioside and TfR molecules – which are considered to reside in detergent resistant and detergent sensitive membrane regions – were used as a negative control. On performing a co-localization experiment, we observed that several yellow pixels were predominant in the superimposed images of CD1d and other proteins (MHC I-HC, MHC II and β_2m) resembling a positive control and indicating confinement of these proteins in the same regions of the membrane (Fig. 3a). Additionally, the cross-correlation coefficient values for these proteins were also remarkably high thus confirming the spatial overlap seen in the images (Fig. 3b).

3.5. Flow-cytometric FRET study among MHC I-HC, β_2m, MHC II and CD1d proteins

To substantiate the findings from co-localization studies, which only indicate juxtaposition of molecules, we performed a cell-by-cell FCET which has been described in detail elsewhere [51], to determine the physical associations of CD1d and other proteins (MHC I-HC, MHC II and β_2m). FRET results suggested that MHC I-HC, β_2m and MHC II proteins were physically associated with CD1d (Fig. 4b). In addition, considerably high FRET efficiencies were also observed between these molecular species (Fig. 4a and b). The association of CD1d with β_2m and MHC proteins (MHC I-HC and MHC II) was also detected by acceptor photobleaching FRET (Supplementary Fig. 1). Interestingly, homoassociation FRET results, a FRET occurring between the same receptors when labeled proportionally with mixtures of different conjugates of the same antibody (independent donor and acceptor conjugates), indicated that both CD1d and MHC II molecules could also exist as dimers or oligomers on the surface of these cells. However, the fluorescence signals were not enough to reliably calculate homoassociation FRET for MHC I-HC and β_2m proteins (Fig. 4c).

3.6. Association of CD1d with GM_1 gangliosides in C1R–CD1d cells

Peptide antigen presenting MHC molecules are associated with lipid enriched membrane regions also called rafts in various types of cells, including lymphocytes [34,54–57]. In fact, such domains are presumed to facilitate compartmentalization, promote protein–protein and lipid–protein interactions on the cell surface [58] and enhance cellular functions, like antigen presentation [28,30,55]. Therefore, we wanted to determine whether CD1d was also enriched in such lipid regions of the plasma membrane. We probed the relationship between CD1d and GM_1 ganglioside, a frequently used marker for rafts. Our result suggested a high degree of overlap between CD1d and GM_1 gangliosides with a cross-correlation coefficient value of ~0.72. A selected example is presented in Fig. 5a, which demonstrates the overlapping regions of CD1d and GM_1 gangliosides in pink.

3.7. Effect of cholesterol depletion and TX100 on CD1d rich membrane regions

The association of CD1d with GM_1 gangliosides was further verified by FRET. Since cholesterol and sphingolipids are the principal components of plasma membrane, we also tested the effect of cholesterol depletion on the observed association between CD1d and GM_1 gangliosides. Simvastatin, a cholesterol synthesis inhibitor [59], and methyl-β-cyclodextrin (MβCD), a known membrane cholesterol extractor from the cell [60], was considered for this purpose. At resting state, a significant FCET result, proving a distinct association, was obtained between CD1d and GM_1 gangliosides. Interestingly, treatment of cells with either MβCD or simvastatin appeared to have a minor effect on the association of CD1d with GM_1 subunits, the effect was not significant at the used concentrations of reagent based on our study (Fig. 5b). Therefore, we performed FCDR experiments to further characterize these CD1d rich regions using detergent TX100. We noted that CD1d rich regions were very sensitive to low concentration of TX100 as depicted in Fig. 6d. Surprisingly, TfR, a non-raft marker abundant in non detergent resistant membrane regions (DRMs) (see also Supplementary Fig. 2), fared better than CD1d in terms of tolerance to TX100 (Fig. 6c and d). MHC II proteins, which are known to partially reside in DRMs, demonstrated superior resistance to TX100 than by TfR proteins (Fig. 6b, c and e). Likewise, the raft marker GM_1 molecules were resilient to TX100 treatment at the employed concentrations. The tolerance to TX100 for these molecules was in the following order: GM_1 > MHC II > TfR > CD1d (Fig. 6). At a typical concentration of 0.013% TX100, the fluorescence intensities of CD1d decreased to ~15%, TfR decreased to ~70%, MHC II decreased to ~80% and that of GM_1 decreased to ~95% within 3 min (Fig. 6e). The maximal decline in fluorescence intensity was observed for CD1d among all tested surface markers. Therefore, mild detergent sensitivity is a specific feature of CD1d proteins on the membrane of B lymphocytes.

3.8. Effect of MβCD and simvastatin on C1R–CD1d cells in iNKT cell activation

Studies, primarily based on murine cell lines have demonstrated contrasting relationships of CD1d with rafts in the plasma membrane. One of the studies suggested that raft localization of CD1d in antigen presenting cells (APCs) is essential for signaling through TCR of NKT cells [28] while another study suggested only a modest effect in the CD1d mediated antigen presentation ability [61] due to MβCD treatment of APCs. Owing to these discrepancies, we performed similar experiments but on human cell lines using primary iNKT cells. We also determined the consequences of simvastatin treatment of B cells on the activation of iNKT cells. We observed that application of 10 mM MβCD (15 min) to C1R–CD1d cells reduced the membrane expression of CD1d proteins (28.8 ± 2.3%, Mean ± S.E.M) in C1R–CD1d cells (Supplementary Fig. 3a); however, this was accompanied by a greater decrease in the production of both cytokines (IFNγ up to 42% and IL4 up to 33%) from iNKT cells. Two millimolar MβCD did not lower the expression of CD1d in C1R–CD1d cells at the used condition and it had only a modest inhibitory effect on the release of IFNγ and IL4 by iNKT cells. Interestingly, the reduction in cytokine production was more prominent in the case of smaller concentration of α-gal (Fig. 7a and b). Furthermore, despite reports on the negative effect of simvastatin in APCs in reducing the cytokine release by iNKT cells [61], we observed that either there is no effect or slight up regulation in the secretion of cytokines (IL4 and IFNγ) by human iNKT cells upon treatment of human C1R–CD1d cells with simvastatin (Fig. 7c and d).

3.9. Simvastatin and MβCD alter membrane protein distribution

Biological membranes are semi-fluid in nature with cholesterol playing a major part in maintaining the integrity of the membrane. Because, cholesterol affects fluidity and bending stiffness of the membrane, we expected alterations in the membrane protein distribution of C1R–CD1d cells when treated with MβCD and simvastatin. We found that both compounds had an effect on the topological arrangement of these proteins in the plasma membrane which means that the drugs had relevant effects on the cell. As demonstrated in Fig. 8, we observed changes in FRET efficiency between CD1d and MHC proteins, especially in the case of simvastatin. Interestingly, the association of MHC I-HC to β_2m is significantly altered in both the cases. Changes in FRET efficiencies between the proteins complemented the observed effect in the decrease of CD1d expression in the cells due to the treatment of these compounds (25.2 ± 1.9%, Mean ± S.E.M, decrease in membrane CD1d expression due to 10 µM simvastatin, Supplementary Fig. 3b). Therefore, both compounds alter the distribution of membrane proteins on the surface of C1R–CD1d cells.

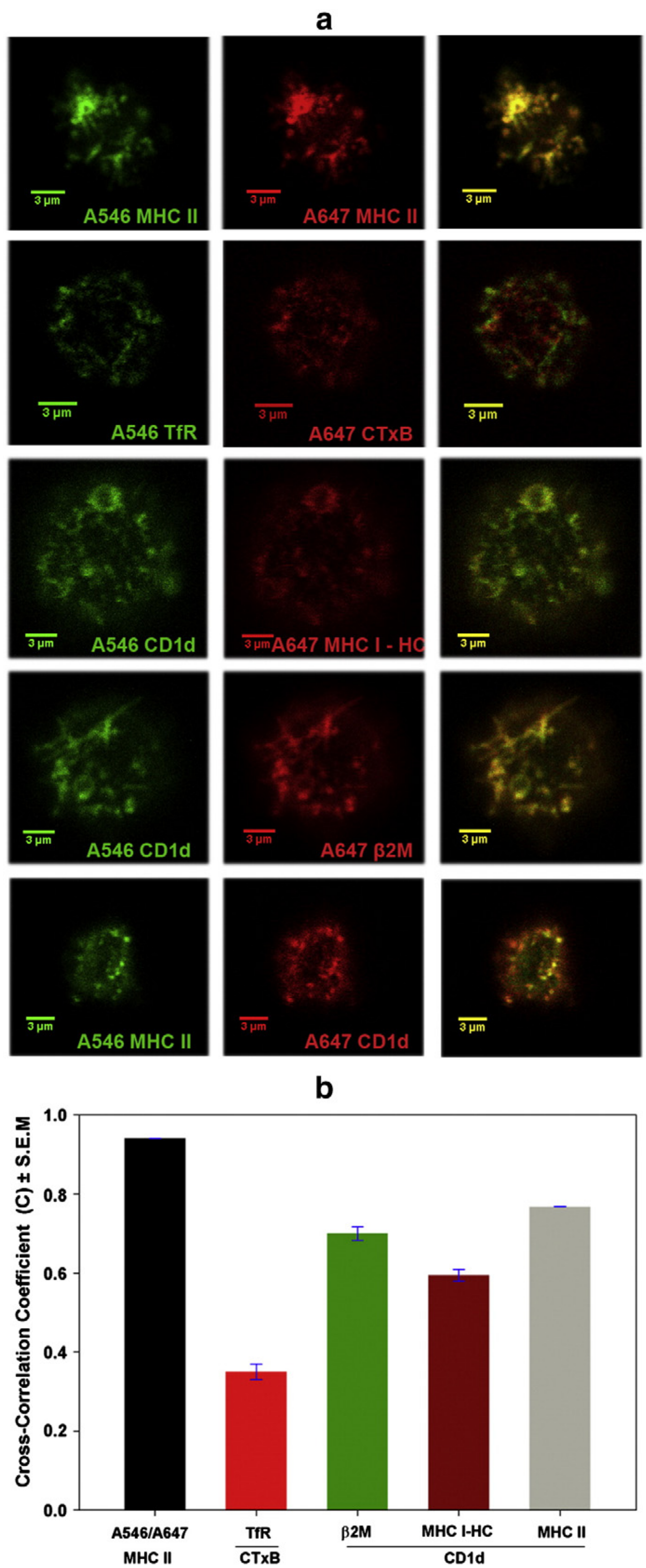

Fig. 3. Co-localization of receptors: a) Representative images for each of the receptors used in co-localization study are presented here. Images at 1.5 µm thickness were scanned from the top of the membrane of a cell. The images were background subtracted in this figure. The first two columns in green and red indicates the images of two different molecular species in pseudo color taken in two different channels of the microscope, and the third column represents the superimposed image for these two channels. The name of the molecules which were imaged is shown on the bottom right corner of each image. Emission from Alexa 546 and Alexa 647 dyes were collected through 560/615 nm BP filter and 650 LP filter respectively. b) Cells were labeled with antibodies against each of the receptors denoted at the x-axis according to the steps described in the Materials and methods section. Thereafter, the top of the membrane was used to record numerous images for each sample from several cells. Next, the co-localization of the two receptors in question was calculated in terms of cross-correlation coefficient value using the LabView program. The first and second row columns indicate positive and negative control respectively. The other columns show the 'C' values between CD1d and other molecules that were probed together. The specific dye conjugated antibodies used are mentioned on the right bottom of each image in Fig. 3a. For a positive control, the same L243 antibody was conjugated with both Alexa 546 and Alexa 647 dyes while CTxB and TfR molecules were used for negative controls.

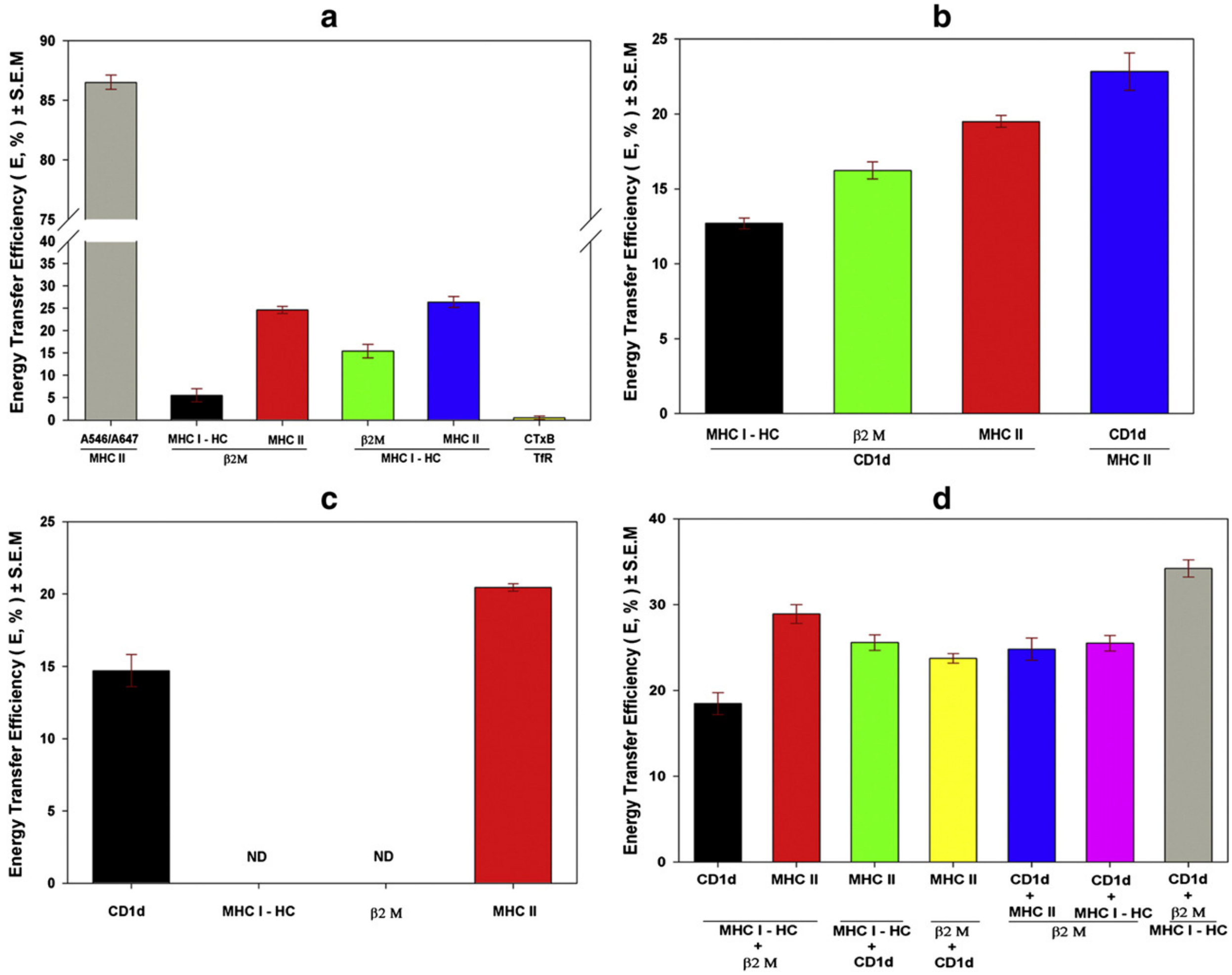

Fig. 4. Flow cytometric FRET (FCET). a) Flow cytometric FRET between the proteins: Columns from left to right represent: Positive Control (Gray) — Both A546 and A647 dyes were conjugated to the same L243 antibody; β_2m served as a donor while MHC I-HC (Black) or MHC II (Red) served as an acceptor; MHC I-HC served as a donor while β2m (Green) or MHC II (Blue) served as an acceptor; CTxB served as a donor while TfR served as an acceptor (Yellow). The FRET pair was always Alexa 546 and Alexa 647 dyes conjugated Mabs except for negative control where CTxB probes were conjugated with Alexa 555 dyes and were used as donor. Flow cytometric FRET between the proteins: b) Columns from left to right represent: CD1d served as an acceptor while MHC I-HC (Black) or β_2m (Green) or MHC II (Red) served as a donor; MHC II served as an acceptor while CD1d (Blue) served as a donor c) Homoassociation Flow cytometric FRET between the proteins: The proteins are described in the x-axis. d) Flow cytometric FRET among three proteins: Columns from left to right represent : (MHC I-HC + β_2m) served as a donor while CD1d (Black) or MHC II (Red) served as an acceptor; (MHC I-HC + CD1d) served as a donor while MHC II (Green) served as an acceptor; (β_2m + CD1d) served as a donor while MHC II (Yellow) served as an acceptor; β_2m served as a donor while (CD1d + MHC II) (Blue) or (CD1d + MHC I-HC) (Pink) served as an acceptor; MHC I-HC served as a donor while (β_2m + CD1d) (Gray) served as an acceptor. (Note: Proteins with '+' mark means the Mabs against these receptors were conjugated to same Alexa dyes. For example 'MHC I-HC + β_2m' means Mabs against MHC I-HC and β_2m were conjugated to Alexa 546 independently and were used in combination as donors for FRET. The same case is also true for two proteins when used as acceptors except that the Mabs against proteins were conjugated to Alexa 647 dyes.).

3.10. Multimolecular complexes of CD1d, MHC and lipid species on the membrane of C1R–CD1d cells

We had no doubts that CD1d and both MHC molecules were associated with each other on the surface of C1R–CD1d cells. Therefore, we assumed that perhaps these molecules can also form a multimolecular protein complex in the membrane of these cells. To demonstrate such possibilities, we performed triple co-localization experiments. The co-occurrence of these proteins was clearly visible, as white pixels, on the superimposed images. Likewise, overlapping regions were also noticed when two of these proteins were imaged together with GM_1 ganglioside (Fig. 9). However, the differential propensity of enrichment in GM_1 rich regions was found between MHC I and MHC II proteins. FRET and co-localization demonstrated that MHC I-HC had a very weak association with GM_1 subunits in comparison with MHC II receptors (Fig. 9, Supplementary Fig. 2 and Supplementary Table 1). Triple co-localization of proteins demonstrating trimolecular complexes of proteins was also supported by our two-color but three-protein FCET experiment. Such a modified FRET setup would help to predict the possibilities of trimolecular complexes in comparison with the conventional two-protein FRET pair which only suggests the interaction of two proteins. With this modified scheme, the FRET efficiency should increase between two proteins in comparison with conventional two protein FRET system when a new protein which is generally a part of trimolecular complex is also included in the FRET pair. In accordance with such assumptions, we observed an increase in the FRET efficiency between any two proteins with the inclusion of a third protein mainly with MHC II as acceptor (Fig. 4d). Thus, considering all lines of evidence, we conclude that multimolecular complexes of CD1d and other proteins (MHC I-HC, β_2m and MHC II) are present in the plasma membrane of these cells, preferably but not exclusively in non-GM_1 regions.

4. Discussion

Non-random distribution patterns of MHC I and MHC II proteins in the plasma membrane have been described in various cell types [32,33,35,36,53,54,56,62]. The modification of these proteins organization was also found to occur during several physiological events, for

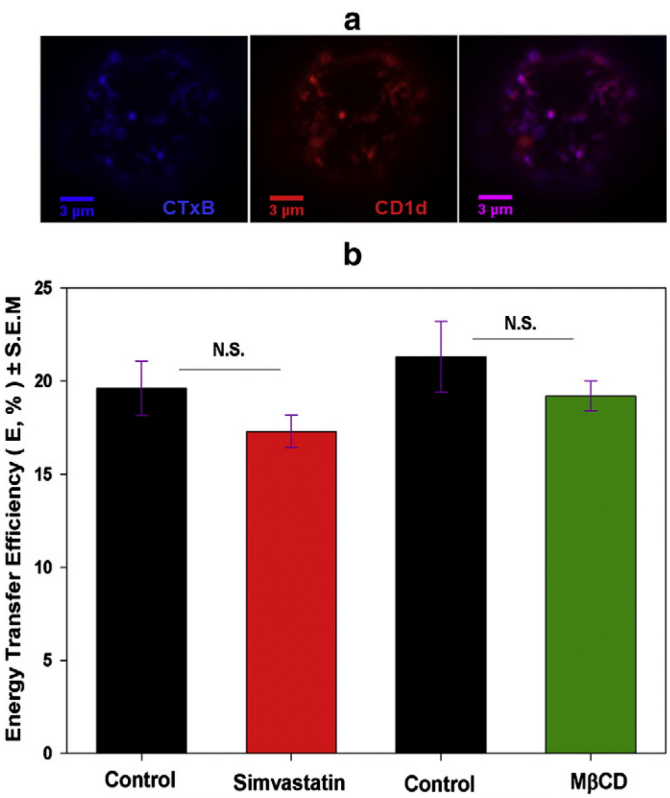

Fig. 5. CD1d and GM_1 ganglioside co-localization: a) Representative image of the distribution of CD1d and GM_1 ganglioside. GM_1 gangliosides were labeled with Alexa 488-CTxB (Blue) and CD1d was labeled with Alexa 647–27.1.9 (Red). The overlay image is presented in the third column with pink pixels indicating co-localization. b) Effect of MβCD and Statin in the Relationship between CD1d and GM_1 ganglioside: C1R–CD1d cells were treated with MβCD and simvastatin as described in the Materials and methods section. Thereafter, the cells were labeled with saturating concentrations of CD1d antibodies and CTxB molecules for FCET experiments. CTxB was used as a donor while CD1d protein was used as an acceptor for FRET. Statistically non-significant '*p*' value is indicated as "N.S." in the figure.

example during immune synapse formation [63,64], diseased condition [65] and cell differentiation stages [66]. However, to our knowledge, no such report is present till now that has demonstrated the quiescent state distribution of CD1d protein in the plasma membrane of B cells. Therefore, using biophysical approaches – including FRET – for the first time we have documented the resting state topological features of CD1d in the plasma membrane of B cells in this study. Quantitative estimation of the number of membrane proteins and evaluation of FRET efficiencies between various protein pairs helped us derive the proximity relationship among MHC I-HC, β_2m, MHC II, and CD1d proteins. We found that CD1d receptors were physically close to MHC I-HC, β_2m and MHC II proteins on the cell-surface. Though the physical association of β_2m and CD1d is not a new phenomenon, our data suggest that the proximity between these two proteins is not entirely dependent on the known non-covalent interactions / or direct binding of these proteins. Rather, the physical association between MHC I and CD1d can also spatially position β_2m, which are mostly bound to MHC I, closer to CD1d proteins (Fig. 4). Since both MHC I-HC and CD1d can interact with β_2m proteins, expectedly there was higher β_2m (~40%) in the plasma membrane of C1R–CD1d "+ve" cells in comparison with C1R–CD1d "−ve" cells. However, flow-cytometric fluorescence histograms and quantitative estimation of membrane proteins in C1R–CD1d "+ve" cells indicated that the total number of β_2m was about 60% of the CD1d proteins expressed in the surface of these cells. Furthermore, almost the entire MHC I-HC (>99%) population was in non-covalent interaction with β_2m based on HC-10 and W6/32 staining of MHC I protein in C1R–CD1d "+ve" cells (Fig. 1b). Therefore, the enhanced number of β_2m in the plasma membrane of C1R–CD1d "+ve" cells represents the only fraction of CD1d that is directly bound with β_2m (~15% of membrane CD1d proteins). The occurrence of very high FRET efficiency between β_2m and CD1d, MHC I-HC and CD1d, MHC II and CD1d proteins also strongly implies that these proteins are the constituents of the same multiprotein complexes. The presence of such supramolecular complexes should also explain why β_2m demonstrated high FRET efficiency with CD1d despite a small fraction of these proteins being bound to CD1d directly (~15%). It thus advances the notion that most of the CD1d (~85%) on the surface of C1R–CD1d cells are not directly bound to β_2m. This might represent the population of CD1d which is immature/ or with poor glycosylation modifications. This observation also complements the earlier reports in which these two isoforms were described by biochemical methods [11,67]. Of note, we did not observe any fluorescence staining due to C3D5 Mab, an antibody considered to bind only CD1d heavy chain, on the plasma membrane of C1R–CD1d cells (data not shown). The inability of this Mab to bind surface CD1d proteins has been noted before [47,68]. This suggests that 27.1.9 and 51.1.3 Mabs can bind both isoforms of CD1d on the cell surface and the non-binding of C3D5 to plasma membrane CD1d proteins rather indicates the inability of C3D5 Mab to recognize the conformation of CD1d heavy chain on the plasma membrane or masking of the epitope recognized by C3D5 or presence of steric hindrance due to multimolecular complexes of proteins on the cell surface. Thus, it remains a challenge to correctly predict the level of expression of both isoforms of CD1d (β_2m-dependent and β_2m-independent forms of CD1d) on the plasma membrane. Nevertheless, both isoforms have been identified in mouse B cells and are found to be capable of activating T cells [69]. It is possible that both isoforms may have distinct functional roles in the activation of T cells. CD1d receptors also displayed homoassociation FRET, suggesting that CD1d proteins can also exist as self clusters in the plasma membrane. Previously, atomic force microscopy (AFM) recognition imaging has revealed the existence of self clusters of CD1d in the plasma membrane of THP1 monocytic cells [70,71]. However, AFM imaging of these cells was carried out in lipid ligand activated monocytic cells. Furthermore, iNKT TCRs were used to investigate CD1d receptors on the plasma membrane. Lipid loading on dendritic cells was found to induce the entry of CD1d receptors to DRM regions [30], therefore, the AFM study should have detected the modified distribution of CD1d receptors unlike the resting state distribution of CD1d receptors. The changes in the plasma membrane distribution of CD1d receptors on lipid loading is also corroborated by the observation that two different lipid antigens produced two different patterns of CD1d distribution on the plasma membrane of THP1 cells [71]. Furthermore, TCRs could only identify lipid bound CD1d receptors. Hence, our study with a specific Mab (27.1.9 clone) which can detect individual CD1d receptors, with or without lipids, is a representation of the quiescent state distribution of CD1d receptors in B cells. We also examined the propensity of CD1d towards lipid species using GM_1 ganglioside at quiescent state. Co-localization and FRET studies indicated the preference of GM_1 rich regions by CD1d proteins. However, cholesterol depleting agents, MβCD and simvastatin, had only a modest effect on the association of CD1d with GM_1 species based on FRET. Plasma membrane cholesterol level decreased by greater than 30% due to both chemicals when monitored by filipin staining (data not shown). These chemicals also alter the topological distribution of membrane proteins (Fig. 8). Therefore, CD1d rich regions show proximity to GM_1 regions and only partial dependence on cholesterol. The observation with MβCD is straightforward because it specifically removes the cholesterol from the plasma membrane, however, the effect of simvastatin might be due to its impact on both cholesterol reduction and isoprenoid pathway. Justifying the secondary effects of simvastatin, it has been reported earlier that simvastatin could decrease antigen presentation by MHC II proteins independent of its inhibitory role in the cholesterol biosynthesis [72]. Here, we also observed an increase in GM_1 surface expression due to simvastatin treatment (data not shown), further indicating it's

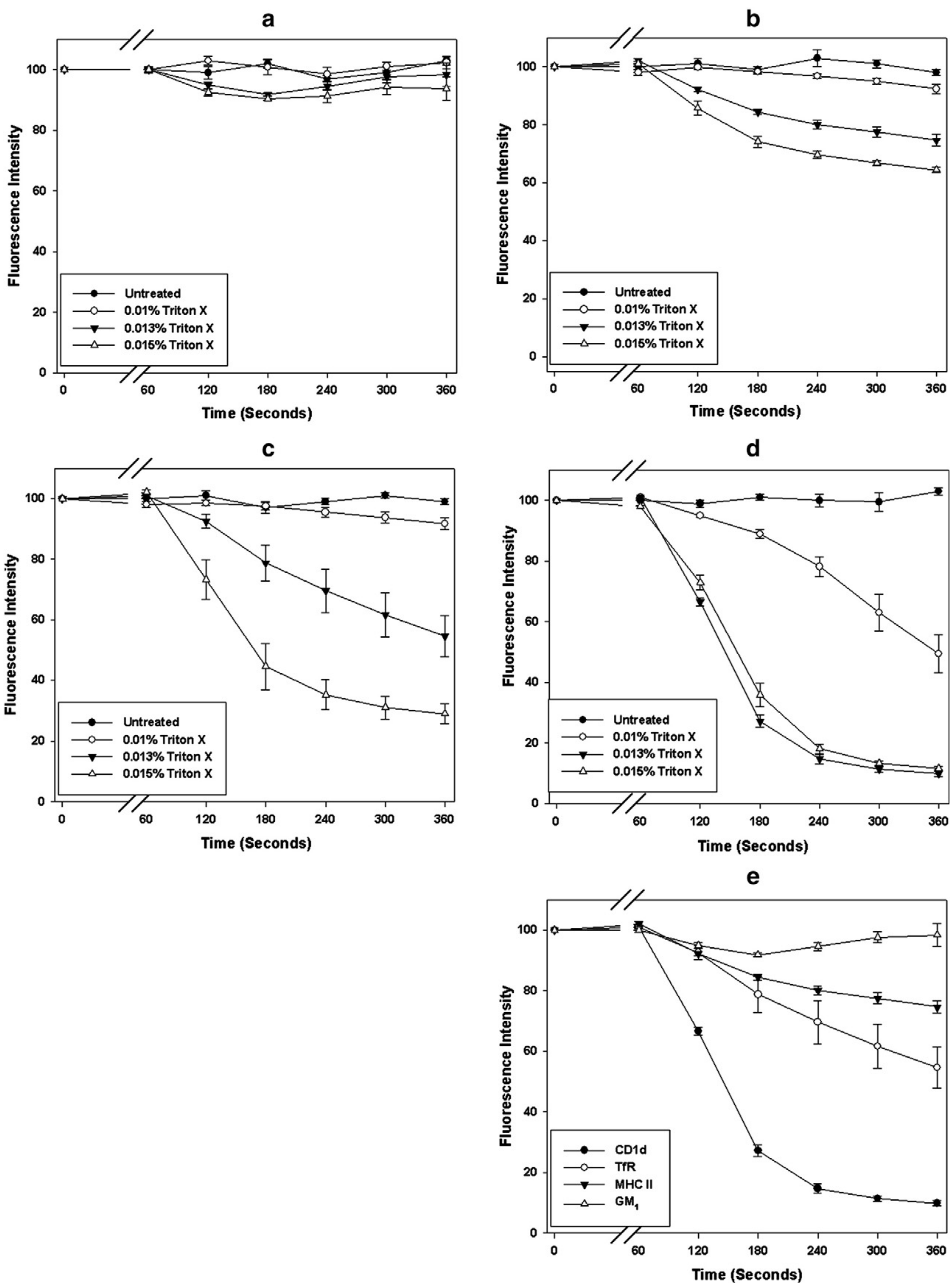

Fig. 6. Flow cytometry based detergent resistance analysis: The response of various surface molecules to TX100 treatment is presented as fluorescence intensity versus time. The samples were prepared by incubating cells with respective probes independently (see Materials and methods also). Non-fixed samples were processed for the measurements. Signals from the TX100 untreated samples were measured for approximately 50 s, then, ice-cold TX100 at various concentrations (untreated, 0.01%, 0.013% and 0.015%) was added to the samples, thereafter, the measurement was continued for approximately 5 min. a) GM_1 subunits b) MHC II proteins c) TfR d) CD1d proteins e) GM_1, MHC II, TfR and CD1d species at 0.013% TX100. The fluorescence intensities were averaged for every 60 seconds except for the first minute where it was averaged for 45 s. The break in the graph (from 45 to 50 s) represents the point of addition of TX100 except for untreated samples where continuous measurements for 6 min were performed. The data for each value is calculated from at least three sets of independent experiments and is presented as Mean $\pm$ S.E.M.

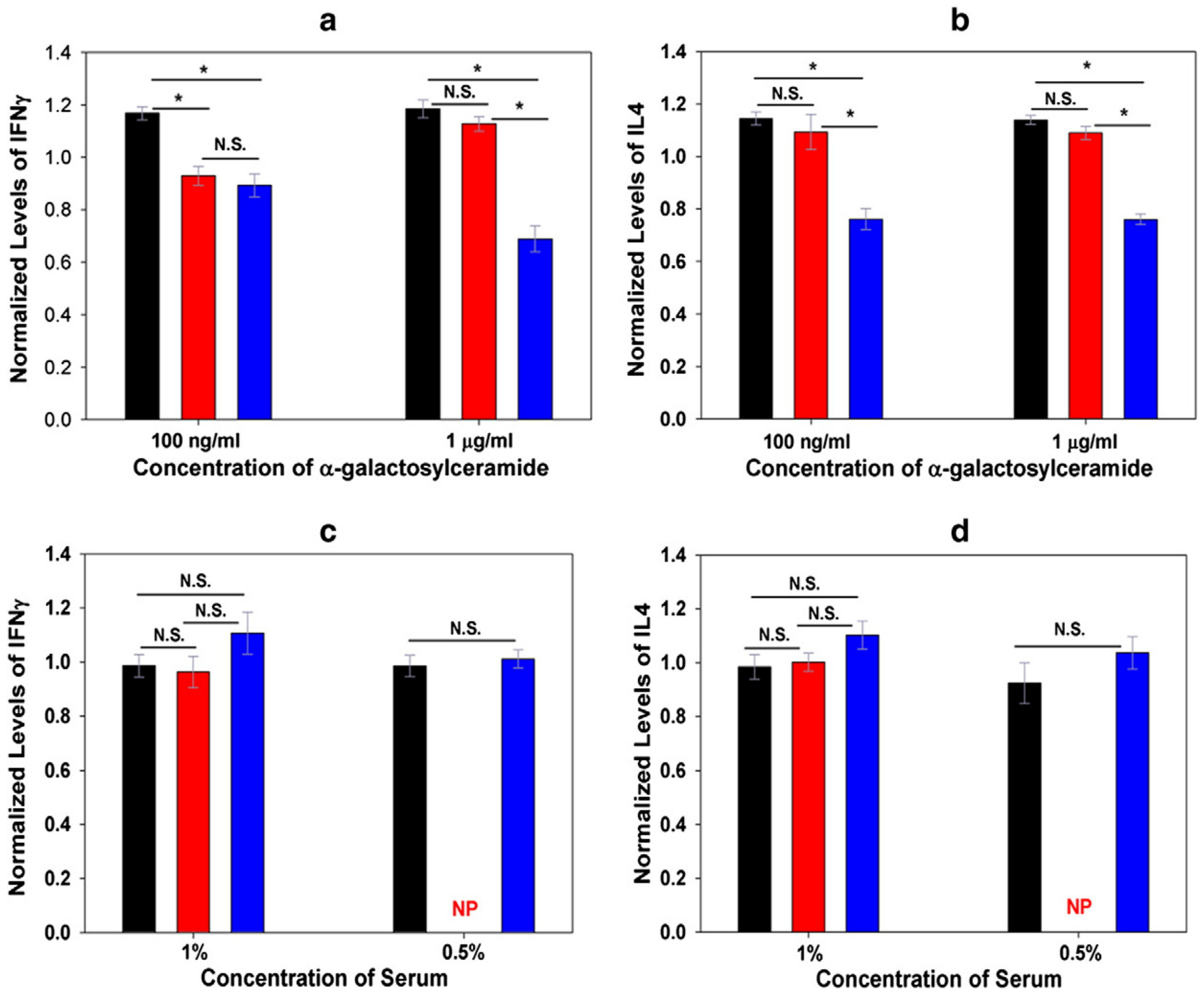

Fig. 7. Effect of MβCD and simvastatin on C1R–CD1d cells in terms of iNKT cell cytokines release: For statistical analyses, either one-way ANOVA together with tukey post-hoc analyses or unpaired *t*-test was done. Statistically non-significant and significant ('$p' < 0.05$) values are indicated by N.S. and '*' symbols respectively. Each datum was normalized by the averaged sum of all data-sets of the particular independent experiment, including values from both control and treated samples, and is represented as Mean ± S.E.M. Three or more independent experiments in triplicates were performed for this study. a) Measurement of IFNγ in the medium after 48 h of co-culture between C1R–CD1d cells and iNKT cells. C1R–CD1d cells were loaded with either 100 ng/ml or 1 μg/ml α-gal for 18 h thereafter it was washed and treated with MβCD. Next, samples were fixed with 1% formaldehyde for 20 min on ice before being used in the co-culture assay. The samples are indicated by the columns in the following colors: Control (Black); 2 mM MβCD treated (Red); 10 mM MβCD treated (Blue). The amount of IFNγ in control samples in Mean ± S.E.M were 1589 ± 402 pg/ml (100 ng/ml α-gal culture) and 1642 ± 412 pg/ml (1 μg/ml α-gal culture). b) Measurement of IL4 in the medium after 48 h of co-culture between C1R–CD1d cells and iNKT cells. C1R–CD1d cells were loaded with either 100 ng/ml or 1 μg/ml α-gal for 18 h thereafter it was washed and treated with MβCD. Next, samples were fixed with 1% formaldehyde for 20 min on ice before being used in the co-culture assay. The samples are indicated by the columns in the following colors: Control (Black); 2 mM MβCD treated (Red); 10 mM MβCD treated (Blue). The amount of IL4 in control samples in Mean ± S.E.M were 551 ± 153 pg/ml (100 ng/ml α-gal culture) and 604 ± 109 pg/ml (1 μg/ml α-gal culture). c) Measurement of IFNγ in the medium after 48 h of co-culture between simvastatin treated C1R–CD1d cells and iNKT cells. C1R–CD1d cells were incubated for 48 h with simvastatin (10 μM, Red and 20 μM, Blue) or without simvastatin (Black) either in 1% NCS media or 0.5% NCS media. Four hours prior to the completion of this incubation period, 250 ng/ml α-gal was added to the C1R–CD1d cells for the loading of iNKT ligand. Next, C1R–CD1d cells were washed extensively and were fixed in 1% formaldehyde for 20 min on ice. Only fixed C1R–CD1d cells were used in the co-culture assay. Experiment with 10 μM simvastatin treatment of C1R–CD1d cells was not performed for 0.5% NCS group. 'NP' means 'Not Performed' in the figure. The amount of IFNγ in control samples in Mean ± S.E.M were 1542 ± 407 pg/ml (1% NCS culture) and 2407 ± 337 pg/ml (0.5% NCS culture). d) Measurement of IL4 in the medium after 48 h of co-culture between simvastatin treated C1R-CD1d cells and iNKT cells. C1R-CD1d cells were incubated for 48 h with simvastatin (10 μM, Red and 20 μM, Blue) or without simvastatin (Black) either in 1% NCS media or 0.5% NCS media. Four hours prior to the completion of this incubation period, 250 ng/ml α-gal was added to the C1R-CD1d cells for the loading of iNKT ligand. Next, C1R-CD1d cells were washed extensively and were fixed in 1% formaldehyde. Only fixed C1R-CD1d cells were used in the co-culture assay. The experiment with 10 μM simvastatin treatment of C1R-CD1d cells was not performed for the 0.5% NCS group. 'NP' means 'Not Performed' in the figure. The amount of IL4 in control samples in Mean ± S.E.M. were 817 ± 145 pg/ml (1% NCS culture) and 1211 ± 236 pg/ml (0.5% NCS culture).

another secondary effect. The partial dependence of CD1d rich regions on cholesterol is also reflected by the co-culture assay between MβCD/simvastatin treated C1R–CD1d cells and iNKT cells. Even on feeding the C1R–CD1d cells with the lipid ligand, α-gal, which induces migration of CD1d to DRM regions, treatment of C1R–CD1d cells with MβCD lead to only a modest decrease in cytokine secretion by iNKT cells. This could be correlated with the partial dependence of CD1d rich regions on cholesterol in the plasma membrane. However, the situation appears to be different for simvastatin because at our experimental conditions we did not see any decrease, rather observed a slight upregulation, in cytokine secretion by iNKT cells despite reduction in the membrane expression of CD1d in C1R-CD1d cells. Simvastatin decreases the level of membrane cholesterol (more than 30% reduction in cholesterol, data not shown) and induces rearrangement of proteins in the plasma membrane. It also seems to affect the expression level of proteins/lipids in the plasma membrane which can modify the fluidity of the membrane. Likewise, simvastatin has been reported to alter the function of small GTPases [73–76] and was also found to disrupt the actin cytoskeleton [77,78] in numerous studies. Actin destabilizing agent and Rho kinase inhibitors were found to enhance antigen presentation by CD1d in murine cells [79]. Therefore the effects of simvastatin on antigen presentation due to decrease in CD1d membrane expression and cholesterol depletion could have been negated by the ability of simvastatin to alter other biological

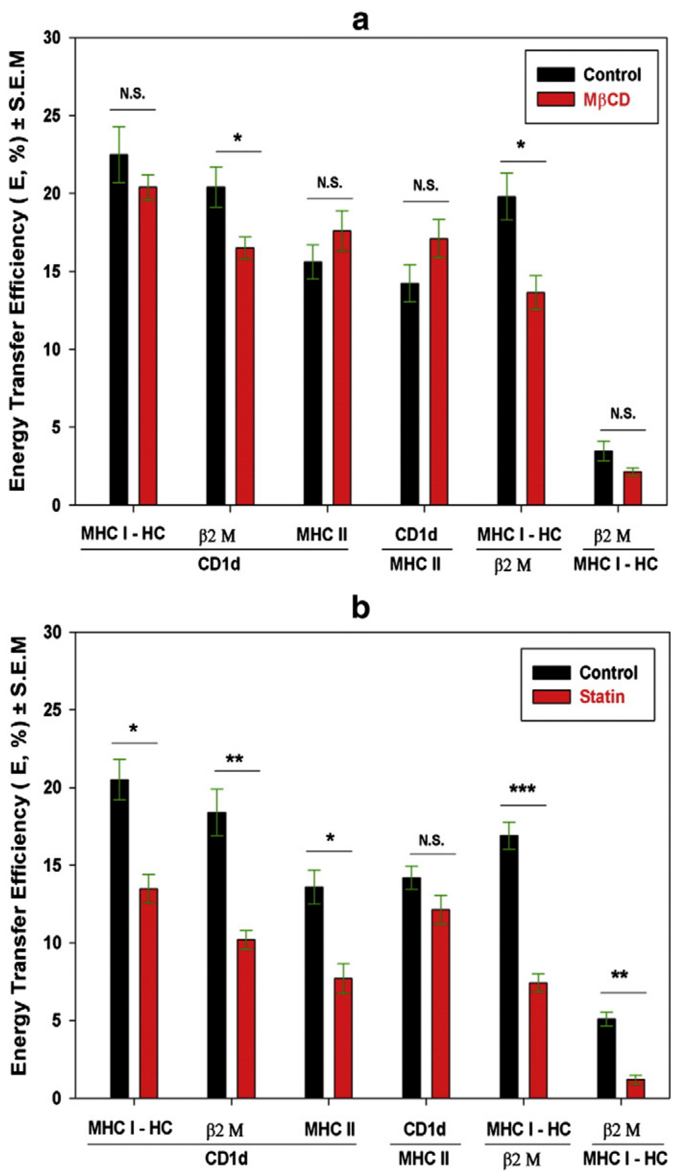

Fig. 8. MβCD and Simvastatin alter membrane protein distribution: C1R–CD1d cells were treated with either MβCD (2 mM, 40 min) or simvastatin (10 μM, 48 h) according to the optimized protocol (Materials and methods). Thereafter, the samples were prepared for FCET experiments accordingly. In the figure, statistically non-significant 'p' value is indicated as 'N.S.', whereas 'p' values <0.05, <0.005, and <0.0005 are indicated by *, **, and *** symbols respectively. a) FRET values for control samples are in black while MβCD treated samples are in red colors. Proteins mentioned below the ticks in x-axis served as a donor while the one that is under the common line served as acceptor for the FRET experiments. b) FRET values for control samples are in black while simvastatin treated samples are in red colors. Proteins mentioned below the ticks in x-axis served as a donor while the ones that are under the common line served as an acceptor for the FRET experiments.

functions including modification of Rho kinase functions and disruption of actin cytoskeleton. However, in our case it would need further investigation to verify such hypothesis and also to demonstrate the importance of isoprenoid pathway, which has been shown to influence CD1d mediated antigen presentation in murine cells [61], in lipid antigen presentation. Further, we performed additional experiments to unravel the specific nature of CD1d enriched membrane regions. Interestingly, CD1d rich regions were highly susceptible to low concentration of TX100 and performed worse than TfR, whereas, GM_1 and MHC II, displayed strong resistance to TX100, as known for DRM associated markers. Therefore, our results suggest that either CD1d proteins are localized in the periphery of GM_1 gangliosides, or are enriched in moderately cholesterol dependent but detergent sensitive membrane regions of the plasma membrane which could be a distinct raft subtype. Similar features of detergent sensitivity by CD1d rich regions have also been noted in other cell types [30,80]. Of note, MHC I proteins are also demonstrated to be present in low cholesterol containing plasma membrane regions [54] which reflects the feature of CD1d rich regions, however, unlike MHC I which is very weakly associated with GM_1 gangliosides, CD1d shows strong GM_1 association, a feature of MHC II proteins. Earlier studies based on various detergents analyses also reinforce the notion that different types of rafts/ or detergent resistant membrane regions might exist [54,81,82]. In addition, recently cholesterol independent sphingolipid domains, ~200 nm in diameter, were highlighted in the plasma membrane of fibroblasts. These sphingolipid domains were primarily dependent on underlying cytoskeletal structures rather than cholesterol [83]. Thus, the nature of CD1d enriched membrane regions needs further characterization especially by comparing it with MHC enriched domains and other raft like domains. Remarkably MHC I, MHC II and CD1d species also demonstrated strong co-occurrence in the plasma membrane. Furthermore, MHC II and CD1d showed markedly high presence in GM_1 rich regions, whereas, MHC I and CD1d scantily co-distributed in GM_1 regions (Fig. 9). Therefore, these molecules as a supramolecular complex are present in the plasma membrane although differences might occur in the abundance of these clusters in GM_1 rich or non-GM_1 rich regions. While unraveling the surface organization features of CD1d receptors, we also found that the plasma membrane expression of CD1d would affect the surface expression of MHC proteins. Since CD1d shares chaperones and invariant chain with MHC proteins, the observed effect might be related to the competition among these proteins for these shared proteins in the intracellular compartments. Such assumption is supported by the fact that cells from invariant chain deficient mice have comparatively low cell surface expression of MHC II proteins and decreased antigen presentation capacity than from normal mice [84,85]. Likewise, expression of CD1a, a subtype of CD1 protein increases the expression of invariant chain in immature dendritic cells [18]. Therefore, investigating the changes in the expression of invariant chain and localization of MHC proteins in the cell under such circumstances might shed light on such features. In the future, it would be of advantage to explore the features of CD1d in the plasma membrane with super-resolution microscopes. These microscopes, like stimulated emission depletion microscopy and near-field scanning optical microscope, are capable of imaging structures beyond the diffraction limit providing resolution below sub 100 nm, therefore, it can provide far more insights into the dynamics and nature of molecular interactions than a conventional confocal microscope. Especially, fluorescence correlation spectroscopy with the aid of these microscopies would be able to dissect the dynamic relationship of CD1d and GM_1 gangliosides or rafts. We believe that elucidating these molecular features of CD1d proteins on the plasma membrane would help us understand the potential ways how CD1d mediated immune pathways could be regulated for therapeutic purpose.

Supplementary data to this article can be found online at http://dx.doi.org/10.1016/j.bbagen.2013.10.030.

Acknowledgements

We would like to thank the support of research grants from the Hungarian Scientific Research Fund (NK 101337); the European Commission grants (LSHC-CT-2005-018914) -ATTACK, MCRTN-CT-2006-036946-2 (IMMUNANOMAP), OTKA NK Research Grant 101337, the New Hungary Development Plan co-financed by the European Social Fund and the European Regional Development Fund (TÁMOP-4.2.2.A-11/1/KONV-2012-0025, TÁMOP-4.2.2-08/1-2008-0019, TÁMOP-4.2.2.A-11/1/KONV-2012-0036 and TÁMOP-4.2.1/B-09/1/KONV-2010-007). We also appreciate TÁMOP-4.2.2/B-10/1-2010-0024 Predoctoral fellowship for supporting Dilip Shrestha. MAE was supported by NIH grants

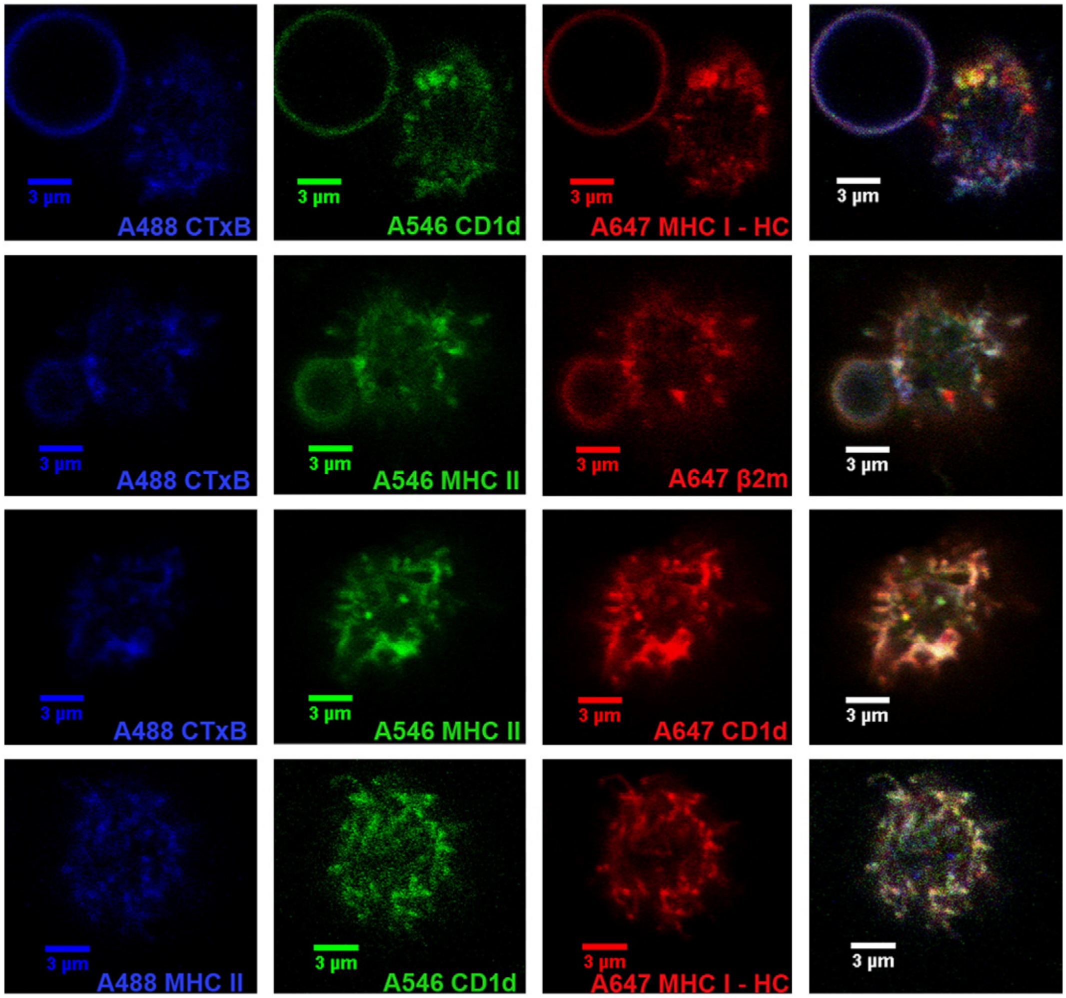

Fig. 9. Triple color labeling experiment: Three molecules from MHC I-HC, β_2m, MHC II, CD1d and GM_1 subunit molecules were labeled simultaneously in similar ways as described in the Materials and methods section. Once prepared, the fixed samples were washed thoroughly, thereafter; the cells were laid on poly-lysine (0.1 mg/ml) coated ibidi chambers. Receptors were then imaged from the top of the membrane using confocal microscope. Specific dyes were used for individual receptors, which are indicated at the right bottom of each image. The last column represents the superimposed image of all the three other columns. Emission from Alexa 488, Alexa 546 and Alexa 647 dyes were collected through 505/550 nm BP filter, 560/615 nm BP filter and 650 LP filter respectively.

CA143748 and CA170194. Lastly, we thank Anita Sárvári from the Department of Biochemistry and Molecular Biology, University of Debrecen for generously arranging and providing PBMC samples and Adrienn Bagosi for her excellent technical assistance.

References

[1] S. Porcelli, M.B. Brenner, J.L. Greenstein, S.P. Balk, C. Terhorst, P.A. Bleicher, Recognition of cluster of differentiation 1 antigens by human CD4–CD8-cytolytic T lymphocytes, Nature 341 (1989) 447–450.
[2] E.M. Beckman, S.A. Porcelli, C.T. Morita, S.M. Behar, S.T. Furlong, M.B. Brenner, Recognition of a lipid antigen by CD1-restricted alpha beta+ T cells, Nature 372 (1994) 691–694.
[3] L. Mori, G. De Libero, T cells specific for lipid antigens, Immunol. Res. 53 (2012) 191–199.
[4] X. Chen, X. Wang, J.M. Keaton, F. Reddington, P.A. Illarionov, G.S. Besra, J.E. Gumperz, Distinct endosomal trafficking requirements for presentation of autoantigens and exogenous lipids by human CD1d molecules, J. Immunol. 178 (2007) 6181–6190.
[5] C.Y. Yu, C. Milstein, A physical map linking the five CD1 human thymocyte differentiation antigen genes, EMBO J. 8 (1989) 3727–3732.
[6] M. Sugita, D.C. Barral, M.B. Brenner, Pathways of CD1 and lipid antigen delivery, trafficking, processing, loading, and presentation, Curr. Top. Microbiol. Immunol. 314 (2007) 143–164.
[7] M. Brigl, M.B. Brenner, CD1: antigen presentation and T cell function, Annu. Rev. Immunol. 22 (2004) 817–890.
[8] C. Gelin, I. Sloma, D. Charron, N. Mooney, Regulation of MHC II and CD1 antigen presentation: from ubiquity to security, J. Leukoc. Biol. 85 (2009) 215–224.
[9] Q. Zhang, R.D. Salter, Distinct patterns of folding and interactions with calnexin and calreticulin in human class I MHC proteins with altered N-glycosylation, J. Immunol. 160 (1998) 831–837.
[10] S.J. Kang, P. Cresswell, Calnexin, calreticulin, and ERp57 cooperate in disulfide bond formation in human CD1d heavy chain, J. Biol. Chem. 277 (2002) 44838–44844.
[11] H.S. Kim, J. Garcia, M. Exley, K.W. Johnson, S.P. Balk, R.S. Blumberg, Biochemical characterization of CD1d expression in the absence of beta2-microglobulin, J. Biol. Chem. 274 (1999) 9289–9295.
[12] V. O'Reilly, S.G. Zeng, G. Bricard, A. Atzberger, A.E. Hogan, J. Jackson, C. Feighery, S.A. Porcelli, D.G. Doherty, Distinct and overlapping effector functions of expanded human CD4+, CD8alpha + and CD4–CD8alpha- invariant natural killer T cells, PLoS One 6 (2011) e28648.
[13] Y.J. Chang, J.R. Huang, Y.C. Tsai, J.T. Hung, D. Wu, M. Fujio, C.H. Wong, A.L. Yu, Potent immune-modulating and anticancer effects of NKT cell stimulatory glycolipids, Proc. Natl. Acad. Sci. U. S. A. 104 (2007) 10299–10304.
[14] M. Sugita, R.M. Jackman, E. van Donselaar, S.M. Behar, R.A. Rogers, P.J. Peters, M.B. Brenner, S.A. Porcelli, Cytoplasmic tail-dependent localization of CD1b antigen-presenting molecules to MIICs, Science 273 (1996) 349–352.
[15] M. Cernadas, M. Cavallari, G. Watts, L. Mori, G. De Libero, M.B. Brenner, Early recycling compartment trafficking of CD1a is essential for its intersection and presentation of lipid antigens, J. Immunol. 184 (2010) 1235–1241.
[16] D.C. Barral, M. Cavallari, P.J. McCormick, S. Garg, A.I. Magee, J.S. Bonifacino, G. De Libero, M.B. Brenner, CD1a and MHC class I follow a similar endocytic recycling pathway, Traffic 9 (2008) 1446–1457.
[17] K.C. Roy, I. Maricic, A. Khurana, T.R. Smith, R.C. Halder, V. Kumar, Involvement of secretory and endosomal compartments in presentation of an exogenous self-glycolipid to type II NKT cells, J. Immunol. 180 (2008) 2942–2950.
[18] I. Sloma, M.T. Zilber, T. Vasselon, N. Setterblad, M. Cavallari, L. Mori, G. De Libero, D. Charron, N. Mooney, C. Gelin, Regulation of CD1a surface expression and antigen presentation by invariant chain and lipid rafts, J. Immunol. 180 (2008) 980–987.

[19] Y. Sagiv, L. Bai, D.G. Wei, R. Agami, P.B. Savage, L. Teyton, A. Bendelac, A distal effect of microsomal triglyceride transfer protein deficiency on the lysosomal recycling of CD1d, J. Exp. Med. 204 (2007) 921–928.

[20] D.G. Rodionov, T.W. Nordeng, K. Pedersen, S.P. Balk, O. Bakke, A critical tyrosine residue in the cytoplasmic tail is important for CD1d internalization but not for its basolateral sorting in MDCK cells, J. Immunol. 162 (1999) 1488–1495.

[21] A.P. Lawton, T.I. Prigozy, L. Brossay, B. Pei, A. Khurana, D. Martin, T. Zhu, K. Spate, M. Ozga, S. Honing, O. Bakke, M. Kronenberg, The mouse CD1d cytoplasmic tail mediates CD1d trafficking and antigen presentation by adaptor protein 3-dependent and -independent mechanisms, J. Immunol. 174 (2005) 3179–3186.

[22] T.S. Devera, L.M. Aye, G.A. Lang, S.K. Joshi, J.D. Ballard, M.L. Lang, CD1d-dependent B-cell help by NK-like T cells leads to enhanced and sustained production of Bacillus anthracis lethal toxin-neutralizing antibodies, Infect. Immun. 78 (2010) 1610–1617.

[23] E. Tonti, G. Galli, C. Malzone, S. Abrignani, G. Casorati, P. Dellabona, NKT-cell help to B lymphocytes can occur independently of cognate interaction, Blood 113 (2009) 370–376.

[24] A. Bosma, A. Abdel-Gadir, D.A. Isenberg, E.C. Jury, C. Mauri, Lipid-antigen presentation by CD1d(+) B cells is essential for the maintenance of invariant natural killer T cells, Immunity 36 (2012) 477–490.

[25] S.J. Kang, P. Cresswell, Regulation of intracellular trafficking of human CD1d by association with MHC class II molecules, EMBO J. 21 (2002) 1650–1660.

[26] S.P. Balk, S. Burke, J.E. Polischuk, M.E. Frantz, L. Yang, S. Porcelli, S.P. Colgan, R.S. Blumberg, Beta 2-microglobulin-independent MHC class Ib molecule expressed by human intestinal epithelium, Science 265 (1994) 259–262.

[27] J. Jayawardena-Wolf, K. Benlagha, Y.H. Chiu, R. Mehr, A. Bendelac, CD1d endosomal trafficking is independently regulated by an intrinsic CD1d-encoded tyrosine motif and by the invariant chain, Immunity 15 (2001) 897–908.

[28] Y.K. Park, J.W. Lee, Y.G. Ko, S. Hong, S.H. Park, Lipid rafts are required for efficient signal transduction by CD1d, Biochem. Biophys. Res. Commun. 327 (2005) 1143–1154.

[29] S. Karmakar, J. Paul, T. De, Leishmania donovani glycosphingolipid facilitates antigen presentation by inducing relocation of CD1d into lipid rafts in infected macrophages, Eur. J. Immunol. 41 (2011) 1376–1387.

[30] W. Peng, C. Martaresche, N. Escande-Beillard, O. Cedile, A. Reynier-Vigouroux, J. Boucraut, Influence of lipid rafts on CD1d presentation by dendritic cells, Mol. Membr. Biol. 24 (2007) 475–484.

[31] G.A. Lang, S.D. Maltsev, G.S. Besra, M.L. Lang, Presentation of alpha-galactosylceramide by murine CD1d to natural killer T cells is facilitated by plasma membrane glycolipid rafts, Immunology 112 (2004) 386–396.

[32] J. Szollosi, S. Damjanovich, M. Balazs, P. Nagy, L. Tron, M.J. Fulwyler, F.M. Brodsky, Physical association between MHC class I and class II molecules detected on the cell surface by flow cytometric energy transfer, J. Immunol. 143 (1989) 208–213.

[33] A. Jenei, S. Varga, L. Bene, L. Matyus, A. Bodnar, Z. Bacso, C. Pieri, R. Gaspar Jr., T. Farkas, S. Damjanovich, HLA class I and II antigens are partially co-clustered in the plasma membrane of human lymphoblastoid cells, Proc. Natl. Acad. Sci. U. S. A. 94 (1997) 7269–7274.

[34] Z. Bacso, L. Bene, L. Damjanovich, S. Damjanovich, INF-gamma rearranges membrane topography of MHC-I and ICAM-1 in colon carcinoma cells, Biochem. Biophys. Res. Commun. 290 (2002) 635–640.

[35] L. Bene, Z. Kanyari, A. Bodnar, J. Kappelmayer, T.A. Waldmann, G. Vamosi, L. Damjanovich, Colorectal carcinoma rearranges cell surface protein topology and density in CD4+ T cells, Biochem. Biophys. Res. Commun. 361 (2007) 202–207.

[36] J. Szollosi, V. Horejsi, L. Bene, P. Angelisova, S. Damjanovich, Supramolecular complexes of MHC class I, MHC class II, CD20, and tetraspan molecules (CD53, CD81, and CD82) at the surface of a B cell line JY, J. Immunol. 157 (1996) 2939–2946.

[37] J. Zemmour, A.M. Little, D.J. Schendel, P. Parham, The HLA-A, B "negative" mutant cell line C1R expresses a novel HLA-B35 allele, which also has a point mutation in the translation initiation codon, J. Immunol. 148 (1992) 1941–1948.

[38] M. Exley, J. Garcia, S.P. Balk, S. Porcelli, Requirements for CD1d recognition by human invariant Valpha24+ CD4−CD8-T cells, J. Exp. Med. 186 (1997) 109–120.

[39] C.J. Barnstable, W.F. Bodmer, G. Brown, G. Galfre, C. Milstein, A.F. Williams, A. Ziegler, Production of monoclonal antibodies to group A erythrocytes HLA and other human cell surface antigens—new tools for genetic analysis, Cell 14 (1978) 9–20.

[40] M. Gauster, A. Blaschitz, G. Dohr, Monoclonal antibody HC10 does not bind HLA-G, Rheumatology (Oxford) 46 (2007) 892–893.

[41] F. Perosa, G. Luccarelli, M. Prete, E. Favoino, S. Ferrone, F. Dammacco, Beta 2-microglobulin-free HLA class I heavy chain epitope mimicry by monoclonal antibody HC-10-specific peptide, J. Immunol. 171 (2003) 1918–1926.

[42] N.J. Stam, H. Spits, H.L. Ploegh, Monoclonal antibodies raised against denatured HLA-B locus heavy chains permit biochemical characterization of certain HLA-C locus products, J. Immunol. 137 (1986) 2299–2306.

[43] N.J. Stam, T.M. Vroom, P.J. Peters, E.B. Pastoors, H.L. Ploegh, HLA-A- and HLA-B-specific monoclonal antibodies reactive with free heavy chains in western blots, in formalin-fixed, paraffin-embedded tissue sections and in cryo-immuno-electron microscopy, Int. Immunol. 2 (1990) 113–125.

[44] L.A. Lampson, C.A. Fisher, J.P. Whelan, Striking paucity of HLA-A, B, C and beta 2-microglobulin on human neuroblastoma cell lines, J. Immunol. 130 (1983) 2471–2478.

[45] P.A. Robbins, E.L. Evans, A.H. Ding, N.L. Warner, F.M. Brodsky, Monoclonal antibodies that distinguish between class II antigens (HLA-DP, DQ, and DR) in 14 haplotypes, Hum. Immunol. 18 (1987) 301–313.

[46] C. Schneider, R. Sutherland, R. Newman, M. Greaves, Structural features of the cell surface receptor for transferrin that is recognized by the monoclonal antibody OKT9, J. Biol. Chem. 257 (1982) 8516–8522.

[47] M. Exley, J. Garcia, S.B. Wilson, F. Spada, D. Gerdes, S.M. Tahir, K.T. Patton, R.S. Blumberg, S. Porcelli, A. Chott, S.P. Balk, CD1d structure and regulation on human thymocytes, peripheral blood T cells B cells and monocytes, Immunology 100 (2000) 37–47.

[48] V. Horejsi, P. Angelisova, V. Bazil, H. Kristofova, S. Stoyanov, I. Stefanova, P. Hausner, M. Vosecky, I. Hilgert, Monoclonal antibodies against human leucocyte antigens. II. Antibodies against CD45 (T200), CD3 (T3), CD43, CD10 (CALLA), transferrin receptor (T9), a novel broadly expressed 18-kDa antigen (MEM-43) and a novel antigen of restricted expression (MEM-74), Folia Biol. (Praha) 34 (1988) 23–34.

[49] G. Vereb, J. Matko, G. Vamosi, S.M. Ibrahim, E. Magyar, S. Varga, J. Szollosi, A. Jenei, R. Gaspar Jr., T.A. Waldmann, S. Damjanovich, Cholesterol-dependent clustering of IL-2Ralpha and its colocalization with HLA and CD48 on T lymphoma cells suggest their functional association with lipid rafts, Proc. Natl. Acad. Sci. U. S. A. 97 (2000) 6013–6018.

[50] G. Vereb, J. Szöllősi, S. Damjanovich, J. Matkó, Exploring membrane microdomains and functional protein clustering in live cells with flow and image cytometric methods, Kluwer Academic / Plenum Publishers, New York, 2004.

[51] G. Szentesi, G. Horvath, I. Bori, G. Vamosi, J. Szollosi, R. Gaspar, S. Damjanovich, A. Jenei, L. Matyus, Computer program for determining fluorescence resonance energy transfer efficiency from flow cytometric data on a cell-by-cell basis, Comput. Methods Programs Biomed. 75 (2004) 201–211.

[52] I. Gombos, Z. Bacso, C. Detre, H. Nagy, K. Goda, M. Andrasfalvy, G. Szabo, J. Matko, Cholesterol sensitivity of detergent resistance: a rapid flow cytometric test for detecting constitutive or induced raft association of membrane proteins, Cytometry A 61 (2004) 117–126.

[53] L. Bene, A. Bodnar, S. Damjanovich, G. Vamosi, Z. Bacso, J. Aradi, A. Berta, J. Damjanovich, Membrane topography of HLA I, HLA II, and ICAM-1 is affected by IFN-gamma in lipid rafts of uveal melanomas, Biochem. Biophys. Res. Commun. 322 (2004) 678–683.

[54] R. Knorr, C. Karacsonyi, R. Lindner, Endocytosis of MHC molecules by distinct membrane rafts, J. Cell Sci. 122 (2009) 1584–1594.

[55] H.A. Anderson, E.M. Hiltbold, P.A. Roche, Concentration of MHC class II molecules in lipid rafts facilitates antigen presentation, Nat. Immunol. 1 (2000) 156–162.

[56] L. Damjanovich, J. Volko, A. Forgacs, W. Hohenberger, L. Bene, Crohn's disease alters MHC-rafts in CD4(+) T-cells, Cytometry A 81 (2012) 149–164.

[57] M. Bouillon, Y. El Fakhry, J. Girouard, H. Khalil, J. Thibodeau, W. Mourad, Lipid raft-dependent and -independent signaling through HLA-DR molecules, J. Biol. Chem. 278 (2003) 7099–7107.

[58] D. Lingwood, K. Simons, Lipid rafts as a membrane-organizing principle, Science 327 (2010) 46–50.

[59] E.S. Istvan, J. Deisenhofer, Structural mechanism for statin inhibition of HMG-CoA reductase, Science 292 (2001) 1160–1164.

[60] R. Zidovetzki, I. Levitan, Use of cyclodextrins to manipulate plasma membrane cholesterol content: evidence, misconceptions and control strategies, Biochim. Biophys. Acta 1768 (2007) 1311–1324.

[61] M.A. Khan, R.M. Gallo, G.J. Renukaradhya, W. Du, J. Gervay-Hague, R.R. Brutkiewicz, Statins impair CD1d-mediated antigen presentation through the inhibition of prenylation, J. Immunol. 182 (2009) 4744–4750.

[62] C. Lagaudriere-Gesbert, S. Lebel-Binay, E. Wiertz, H.L. Ploegh, D. Fradelizi, H. Conjeaud, The tetraspanin protein CD82 associates with both free HLA class I heavy chain and heterodimeric beta 2-microglobulin complexes, J. Immunol. 158 (1997) 2790–2797.

[63] H. de la Fuente, M. Mittelbrunn, L. Sanchez-Martin, M. Vicente-Manzanares, A. Lamana, R. Pardi, C. Cabanas, F. Sanchez-Madrid, Synaptic clusters of MHC class II molecules induced on DCs by adhesion molecule-mediated initial T-cell scanning, Mol. Biol. Cell 16 (2005) 3314–3322.

[64] E.M. Hiltbold, N.J. Poloso, P.A. Roche, MHC class II-peptide complexes and APC lipid rafts accumulate at the immunological synapse, J. Immunol. 170 (2003) 1329–1338.

[65] L. Damjanovich, J. Volko, A. Forgacs, W. Hohenberger, L. Bene, Crohn's disease alters MHC-rafts in CD4+ T-cells, Cytometry A 81 (2012) 149–164.

[66] N. Setterblad, C. Roucard, C. Bocaccio, J.P. Abastado, D. Charron, N. Mooney, Composition of MHC class II-enriched lipid microdomains is modified during maturation of primary dendritic cells, J. Leukoc. Biol. 74 (2003) 40–48.

[67] K. Somnay-Wadgaonkar, A. Nusrat, H.S. Kim, W.P. Canchis, S.P. Balk, S.P. Colgan, R.S. Blumberg, Immunolocalization of CD1d in human intestinal epithelial cells and identification of a beta2-microglobulin-associated form, Int. Immunol. 11 (1999) 383–392.

[68] J. Liu, D. Shaji, S. Cho, W. Du, J. Gervay-Hague, R.R. Brutkiewicz, A threonine-based targeting signal in the human CD1d cytoplasmic tail controls its functional expression, J. Immunol. 184 (2010) 4973–4981.

[69] M. Amano, N. Baumgarth, M.D. Dick, L. Brossay, M. Kronenberg, L.A. Herzenberg, S. Strober, CD1 expression defines subsets of follicular and marginal zone B cells in the spleen: beta 2-microglobulin-dependent and independent forms, J. Immunol. 161 (1998) 1710–1717.

[70] M. Duman, M. Pfleger, R. Zhu, C. Rankl, L.A. Chtcheglova, I. Neundlinger, B.L. Bozna, B. Mayer, M. Salio, D. Shepherd, P. Polzella, M. Moertelmaier, G. Kada, A. Ebner, M. Dieudonne, G.J. Schutz, V. Cerundolo, F. Kienberger, P. Hinterdorfer, Improved localization of cellular membrane receptors using combined fluorescence microscopy and simultaneous topography and recognition imaging, Nanotechnology 21 (2010) 115504.

[71] M. Duman, L.A. Chtcheglova, R. Zhu, B.L. Bozna, P. Polzella, V. Cerundolo, P. Hinterdorfer, Nanomapping of CD1d-glycolipid complexes on THP1 cells by using simultaneous topography and recognition imaging, J. Mol. Recognit. 26 (2013) 408–414.

[72] R. Ghittoni, G. Napolitani, D. Benati, C. Ulivieri, L. Patrussi, F. Laghi Pasini, A. Lanzavecchia, C.T. Baldari, Simvastatin inhibits the MHC class II pathway of antigen presentation by impairing Ras superfamily GTPases, Eur. J. Immunol. 36 (2006) 2885–2893.

[73] B.M. Maher, T.N. Dhonnchu, J.P. Burke, A. Soo, A.E. Wood, R.W. Watson, Statins alter neutrophil migration by modulating cellular Rho activity—a potential mechanism for statins-mediated pleotropic effects? J. Leukoc. Biol. 85 (2009) 186–193.
[74] A.M. deCathelineau, G.M. Bokoch, Inactivation of rho GTPases by statins attenuates anthrax lethal toxin activity, Infect. Immun. 77 (2009) 348–359.
[75] G. Martin, H. Duez, C. Blanquart, V. Berezowski, P. Poulain, J.C. Fruchart, J. Najib-Fruchart, C. Glineur, B. Staels, Statin-induced inhibition of the Rho-signaling pathway activates PPARalpha and induces HDL apoA-I, J. Clin. Invest. 107 (2001) 1423–1432.
[76] R. Ghittoni, L. Patrussi, K. Pirozzi, M. Pellegrini, P.E. Lazzerini, P.L. Capecchi, F.L. Pasini, C.T. Baldari, Simvastatin inhibits T-cell activation by selectively impairing the function of Ras superfamily GTPases, FASEB J. 19 (2005) 605–607.
[77] M. Copaja, D. Venegas, P. Aranguiz, J. Canales, R. Vivar, Y. Avalos, L. Garcia, M. Chiong, I. Olmedo, M. Catalan, L. Leyton, S. Lavandero, G. Diaz-Araya, Simvastatin disrupts cytoskeleton and decreases cardiac fibroblast adhesion, migration and viability, Toxicology 294 (2012) 42–49.
[78] M. Pozo, R. de Nicolas, J. Egido, J. Gonzalez-Cabrero, Simvastatin inhibits the migration and adhesion of monocytic cells and disorganizes the cytoskeleton of activated endothelial cells, Eur. J. Pharmacol. 548 (2006) 53–63.
[79] R.M. Gallo, M.A. Khan, J. Shi, R. Kapur, L. Wei, J.C. Bailey, J. Liu, R.R. Brutkiewicz, Regulation of the actin cytoskeleton by Rho kinase controls antigen presentation by CD1d, J. Immunol. 189 (2012) 1689–1698.
[80] J.S. Im, P. Arora, G. Bricard, A. Molano, M.M. Venkataswamy, I. Baine, E.S. Jerud, M.F. Goldberg, A. Baena, K.O. Yu, R.M. Ndonye, A.R. Howell, W. Yuan, P. Cresswell, Y.T. Chang, P.A. Illarionov, G.S. Besra, S.A. Porcelli, Kinetics and cellular site of glycolipid loading control the outcome of natural killer T cell activation, Immunity 30 (2009) 888–898.
[81] D. Locke, J. Liu, A.L. Harris, Lipid rafts prepared by different methods contain different connexin channels, but gap junctions are not lipid rafts, Biochemistry 44 (2005) 13027–13042.
[82] K. Roper, D. Corbeil, W.B. Huttner, Retention of prominin in microvilli reveals distinct cholesterol-based lipid micro-domains in the apical plasma membrane, Nat. Cell Biol. 2 (2000) 582–592.
[83] J.F. Frisz, H.A. Klitzing, K. Lou, I.D. Hutcheon, P.K. Weber, J. Zimmerberg, M.L. Kraft, Sphingolipid domains in the plasma membranes of fibroblasts are not enriched with cholesterol, J. Biol. Chem. 288 (2013) 16855–16861.
[84] E.K. Bikoff, L.Y. Huang, V. Episkopou, J. van Meerwijk, R.N. Germain, E.J. Robertson, Defective major histocompatibility complex class II assembly, transport, peptide acquisition, and CD4+ T cell selection in mice lacking invariant chain expression, J. Exp. Med. 177 (1993) 1699–1712.
[85] E.A. Elliott, J.R. Drake, S. Amigorena, J. Elsemore, P. Webster, I. Mellman, R.A. Flavell, The invariant chain is required for intracellular transport and function of major histocompatibility complex class II molecules, J. Exp. Med. 179 (1994) 681–694.